PHYSICAL REVIEW C VOLUME 21, NUMBER 1 JANUARY 1980

Pion-nucleus scattering using finite binding potentials

M. Silver and N. Austern
University of Pittsburgh, Pittsburgh, Pennsylvania 15260
(Received 30 May 1979)

A nonperturbative treatment of finite binding potentials in pion-bound nucleon scattering is developed. Coupled differential equations in configuration space are derived from a model wave function broken into two parts. Coordinates from the source of binding to the pion and to the nucleon are used in the elastic channel, while pion-nucleon center-of-mass coordinates are used for the excited channels. The excited channel equations are solved in closed form using a separable nonlocal pion-nucleon interaction. When the solution is inserted into the elastic channel equation, a relativistically modified single-particle equation for the elastically scattered meson is derived, which features an optical potential with both local and nonlocal parts. This model is used in conjunction with first order multiple scattering theory to construct pion-nucleus scattering. In the present application of the model the assumed pion-nucleon interaction is taken to be s wave with threshold p-wave behavior. The region around the 33 resonance is numerically studied for both the three-body model and for pions on ^{16}O. A consistent, inclusive treatment of many effects familiar from earlier work is obtained. Results from the three-body calculation show that the peak cross section is shifted upwards by about the binding energy of the struck nucleon. However, nonlinear effects drive the peak downwards when the three-body model is incorporated in the pion-nucleus formalism, so that several bound nucleons simultaneously scatter the meson. Effects of this kind are not expected to be sensitive to the use of an artificial $l = 0$ πN interaction. Resonances caused by the binding potential are found to be important in both the three-body and the π-^{16}O calculations. This suggests significant corrections to an impulse approximation approach.

[NUCLEAR REACTIONS $^{16}O(\pi,\pi)$, three-body model of π-nucleon interaction, $\sigma_T(E)$ calculated.]

I. INTRODUCTION

Most treatments of pion-nucleus scattering are based on some form of the impulse approximation, in which the elementary scattering event is the collision of the pion with individual target nucleons that are treated as free, with at most some energy or momentum correction for their location in the nucleus. In this procedure, multiple scattering theory is used to combine individual amplitudes for pion-nucleon (πN) scattering, to obtain an optical potential for pion-nucleus scattering.[1-18] Techniques such as the frozen-nucleus approximation sometimes allow partial summation of higher-order terms of the multiple scattering series.[19-24]

There has also been some interest in multiple scattering theories that are based on collisions of the meson with nucleons that are bound by the shell model potential of the nucleus.[25-37] In such an approach the elementary event of the multiple scattering procedure is a three-body collision, in which the binding potential and the meson-nucleon interaction act simultaneously. However, previous calculations of three-body theories for bound nucleons have used harmonic oscillator binding potentials, which do not allow ejection of the nucleon from the nucleus, and they have introduced perturbative treatments of the binding potentials at intermediate stages of calculation.[28-35,37]

The present article considers a nonperturbative evaluation of a model three-body Schrödinger equation for the scattering of a meson by a bound nucleon: The nucleon is bound to a fixed origin by a Woods-Saxon potential and the meson interacts with the nucleon by a single-term separable potential that has angular momentum l_0. Although the formal development of the model treats l_0 as a general parameter, the present evaluation is limited to the artificial special case $l_0 = 0$, as in several previous three-body studies.[28-31] However, the calculation is made more realistic by forcing the free phase shift for our $l_0 = 0$ interaction to match the known energy dependence of the $l = 1$, 33-phase shift. The model is applied to the scattering of pions by ^{16}O, in the resonance region, using first-order multiple scattering theory to combine contributions from individual struck nucleons. The Coulomb potential is omitted. Explicit coupling to nuclear spins is omitted. Further details of the present work may be found in Ref. 38.

The Schrödinger equation is solved in configuration space, to allow an easy discussion of the Woods-Saxon wave functions and of the various optical potentials that are derived. We work in

the laboratory coordinate system, in which the origin of the shell model potential is held fixed.

Two sets of position coordinates are used: The $\vec{r}, \vec{s}$ coordinates from the source of binding to the nucleon and the meson, respectively, and the $\vec{R}, \vec{\rho}$ coordinates to the pion-nucleon center of mass and between the two particles, respectively (see Fig. 1). Although these are the same coordinates that would appear in a Faddeev configuration space formulation, we do not proceed by that method. The difficulties of a Faddeev approach for reactions with a large nucleus are familiar.[39] Each set of coordinates is associated with many partial waves. The multiplicity of couplings of these partial waves in the Faddeev procedure leads to an excessive number of coupled equations. (Of course, Faddeev calculations of meson-deuteron scattering converge much better.[40-49])

An approximate system of coupled equations is adopted instead, based on the observation that the $\vec{r}, \vec{s}$ coordinates are primarily required for the few shell model bound states of the target nucleons, and especially for the nuclear ground state, which defines the entrance channel. On the other hand, the $\vec{R}, \vec{\rho}$ coordinates are well adapted for the analysis of effects caused by the strong meson-nucleon interaction. We therefore use projection operators to separate the wave function into two parts: The entrance channel part is described in $\vec{r}, \vec{s}$ coordinates, and the remainder of the wave function, especially the three-body breakup channels, is described in $\vec{R}, \vec{\rho}$ coordinates. This separation of the wave function allows the development of a series of approximations that lead to manageable coupled equations. (Similar approximations appear in articles by Lenz and co-workers.[50,51]) The equations based on continuum excited states of the target nucleon are readily solved, leading to a single complicated Schrödinger equation for the elastic channel, with an optical potential that is summed over intermediate nucleon excited states.

The three-body analysis of pion bound nucleon scattering is developed in Sec. II, and the approximations used to obtain manageable coupled equations are discussed. Approximations taken from first-order multiple scattering theory are applied in Sec. III, to express scattering from a closed shell target nucleus as a sum over three-body collisions with the individual nucleons. In particular, the optical potential is computed as a sum over occupied nucleon orbitals. (These separate contributions to the optical potential interfere with each other in a complicated nonlinear fashion when the Schrödinger equation for elastic scattering is solved. We see later that several familiar effects in pion-nucleus scattering are caused by this nonlinearity.)

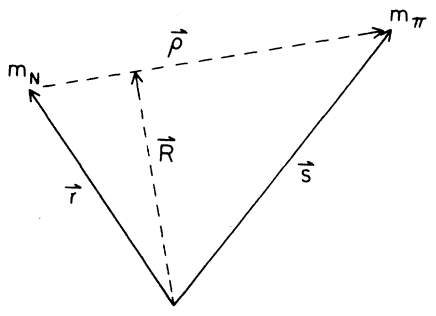

FIG. 1. The two sets of coordinates in the three-body model. The source of binding is fixed.

Section IV presents the potentials used in our calculation. Section V outlines the calculational details necessary to reduce the formal expressions of Secs. II and III to tractable equations for numerical solution. Relativistic modifications are introduced. Section VI presents and discusses results for meson scattering by a single bound nucleon and by ^{16}O. We measure the effects of binding by changes in the location of the total cross section maximum in the 33-resonance region. We also examine the elastic and reaction contributions to the total cross section and look for changes in the magnitude and shape of the cross sections. Section VII is a brief statement of conclusions. The Appendix discusses limiting approximations of the optical potential for the closure limit, which is equivalent to an impulse approach, and for the zero-binding limit.

II. THREE-BODY MODEL

A. Configuration space method

In this section a technique for solving pion scattering from a nucleon bound in a finite potential is given. A simplified presentation—nonrelativistic kinematics, spinless nucleon, and a fixed potential that supports only one bound orbital—will exhibit the features of the method.

We place the origin of coordinates at the site of the binding potential and introduce two sets of coordinates. One is the fixed or $\vec{r}, \vec{s}$ system where $\vec{r}$ locates the nucleon and $\vec{s}$ the meson, the other is the center-of-mass or $\vec{R},\vec{\rho}$ system where $\vec{R}$ locates the πN center of mass and $\vec{\rho}$ is the relative πN displacement, see Fig. 1. The transformations between the two systems are given by

$$\vec{R} = \overline{\nu}\vec{r} + \nu\vec{s}\,, \quad \vec{\rho} = \vec{s} - \vec{r} \tag{1a}$$

or

$$\vec{r} = \vec{R} - \nu\vec{\rho}\,, \quad \vec{s} = \vec{R} + \overline{\nu}\vec{\rho}\,, \tag{1b}$$

with

$$\nu = m_\pi/(m_N + m_\pi), \quad \bar{\nu} = 1 - \nu . \tag{1c}$$

The time independent Schrödinger equation for this model is

$$(E - K - U)\Psi = V\Psi , \tag{2}$$

where Ψ is the complete wave function for the pion and nucleon motion relative to a fixed core, K is the kinetic energy operator for both particles, $U(r)$ is the nucleon binding potential, and $V(\rho)$ is the pion-nucleon interaction. Equation (2) does not contain any meson-core interaction. However, the effects of such an interaction do appear when we consider scattering by a nucleus, when all the nucleons can affect the meson simultaneously. We approach the solution of Eq. (2) in configuration space. The kinetic energy operator K separates in either the $\vec{r}, \vec{s}$ or $\vec{R}, \vec{\rho}$ coordinates.

To solve Eq. (2) in configuration space suggests choosing between the two sets of orthogonal coordinates $\vec{r}, \vec{s}$ or $\vec{R}, \vec{\rho}$. However, U is a function of r—a member of the first coordinate set—while V is a function of ρ—a member of the other coordinate set. We particularly need the $\vec{R}, \vec{\rho}$ coordinate set to take advantage of the separable πN interaction that is introduced later. However, we also require a correct description of the entrance channel, for which the nucleon is in its ground state. This is best done in $\vec{r}, \vec{s}$ coordinates because the nucleon ground wave function is an eigensolution of the binding potential $U(r)$. To resolve this conflict, we introduce projection operators that split Eq. (2) into two coupled equations: One isolates the entrance channels and is solved in $\vec{r}, \vec{s}$ coordinates, the other features nucleon excitations caused by V and is solved in $\vec{R}, \vec{\rho}$ coordinates.

The nucleon ground state projector P is expressed in terms of nucleon wave functions ψ_ϵ, which satisfy

$$[\epsilon - U(r) - K_{\vec{r}}]\psi_\epsilon(\vec{r}) = 0 . \tag{3a}$$

Then P becomes

$$P(\vec{r}, \vec{r}') = \psi_0(\vec{r}) \int d\vec{r}'\psi_0^*(\vec{r}') \ldots , \tag{4a}$$

where ψ_0 is the ground state wave function. We define

$$Q = 1 - P . \tag{4b}$$

Both P and Q commute with $K + U$. We also need nucleonlike wave functions $\bar{\psi}_\epsilon(\vec{R})$, defined by

$$[\epsilon - U(R) - K_{\vec{R}}]\bar{\psi}_\epsilon(\vec{R}) = 0 , \tag{3b}$$

where $K_{\vec{R}}$ contains the total mass—pion plus nucleon—instead of only the nucleon mass as in $K_{\vec{r}}$.

In terms of the projection operators, Eq. (2) becomes

$$(E - K - U)P\Psi = PV\Psi , \tag{5a}$$

$$(E - K - U)Q\Psi = QV\Psi . \tag{5b}$$

The first equation is solved in $\vec{r}, \vec{s}$ coordinates to allow correct handling of the incoming flux. The second equation is solved in $\vec{R}, \vec{\rho}$ coordinates to accommodate the ρ dependence of the πN interaction.

Therefore, we expand the full wave function Ψ in two parts, each in a different coordinate system. We adopt the form

$$\Psi = \psi_0(\vec{r})F(\vec{s}) + \left[\bar{\psi}_0(\vec{R})G_0(\vec{\rho}) + \int_0^\infty d\epsilon\bar{\psi}_\epsilon(\vec{R})G_\epsilon(\vec{\rho})\right] . \tag{6}$$

Here the $\bar{\psi}_0(\vec{R})G_0(\vec{\rho})$ piece is a bound-state counter term that is introduced because eigenstates constructed in one set of coordinates are not necessarily orthogonal to eigenstates constructed in the other coordinate set. We adjust the factor $G_0(\rho)$ to produce orthogonality between $\psi_0(\vec{r})F(\vec{s})$ and the expression in brackets. This means the first term in Ψ assumes the meaning of $P\Psi$ and the part in brackets $Q\Psi$. That is, the overlap of $\psi_0(\vec{r})$ with the terms in brackets is compelled to vanish:

$$\int d\vec{r}\psi_0^*(\vec{r})\bar{\psi}_0(\vec{R})G_0(\vec{\rho}) + \int d\vec{r}\psi_0^*(\vec{r}) \times \int_0^\infty d\epsilon\bar{\psi}_\epsilon(\vec{R})G_\epsilon(\vec{\rho}) = 0 . \tag{7}$$

This equation of orthogonality now implies that $Q\Psi$ fulfills the required outgoing boundary condition.

An explicit calculation of the bound-state counter term[38] shows that it resembles the $J = 0$ partial wave of the elastic-channel wave function $F(\vec{s})$, but it has a much smaller amplitude. For small $\nu\rho$ the magnitude is reduced by the approximate orthogonality of $\psi_0(\vec{r})$ and $\bar{\psi}_\epsilon(\vec{R})$. At large ρ, integration over the oscillations of $\bar{\psi}_\epsilon(\vec{R})$ reduces the counter term. Hereafter, this term is dropped.

It is interesting to note how free pion-nucleon scattering can be recovered from the system of coupled equations described here. Although the binding potential cannot go to zero without destroying the structure of the coupled equations, we can let the potential become weak enough so that the nucleon binding energy goes to zero. The formal structure of the equations remains intact, but now as the energy goes to zero the ground state nucleon wave function occupies more and more volume outside the range of $U(r)$; i.e., the nucleon becomes more and more free. In turn, upon encountering the pion, the nearly free nucleon recoils and is scattered out of the elastic channel.

The recoiling nucleon is described by the $Q\Psi$ part of the wave function and its motion is governed by the second coupled equation (5b). As the binding potential becomes weak, U in (5b) is of diminished importance and this equation takes on the appearance of the relative motion Schrödinger equation for free πN scattering (with the remaining coupling necessary to describe the incoming flux). A more detailed description of the free scattering limit is given in the Appendix.

To solve the coupled equations, we premultiply Eq. (5a) by $\psi_0(\vec{r})$ and integrate over $\vec{r}$, to obtain

$$(E-\epsilon_0-K_{\vec{s}})F(\vec{s})=(\psi_0(\vec{r}),\, V(\vec{\rho})\psi_0(\vec{r})F(\vec{s}))+(\psi_0(\vec{r}),\, V(\vec{\rho})\int_0^\infty d\epsilon\,\bar{\psi}_\epsilon(\vec{R})G_\epsilon(\vec{\rho}))\,. \tag{8a}$$

Premultiply Eq. (5b) by $\bar{\psi}_\epsilon(\vec{R})$ and integrate over $\vec{R}$, to obtain

$$(E-\epsilon-K_{\vec{\rho}})G_\epsilon(\vec{\rho})=(\bar{\psi}_\epsilon(\vec{R}),\, Q(\vec{r},\vec{r}')V(\vec{\rho}')\Psi)+(\bar{\psi}_\epsilon(\vec{R}),\, [U(r)-U(R)]Q\Psi)\,. \tag{8b}$$

The derivation of (8b) requires that $U(r)$ in the left-hand side of (5b) be replaced by $U(R)$, thus allowing the insertion of the eigenvalue ϵ for the nucleonlike Hamiltonian $U(R)+K_{\vec{R}}$ when premultiplied by $\bar{\psi}_\epsilon(R)$ in (8b). This step replaces one three-body continuum by another. Instead of $\vec{r}$, $\vec{s}$, Eq. (8b) uses the more convenient variables $\vec{R}$, $\vec{\rho}$ and the associated outgoing boundary conditions. However, this simplification of the structure of (8b) introduces what we call the frame potential, $U(r)$-$U(R)$, on the right-hand side of (8b).

Another complication in (8b) is the presence of the projector $Q(\vec{r},\vec{r}')$, which we replace by $1-P(\vec{r},\vec{r}')$. Both the frame potential term and the contribution from $P(\vec{r},\vec{r}')$ are now seen to be small corrections in (8b), for similar reasons. Both correction terms are negligible at the important point $\rho=0$, which dominates the subsequent application of $G_\epsilon(\vec{\rho})$ in (8a); also, both correction terms have rather smooth behavior at large ρ, therefore they do not alter the outgoing boundary conditions for $G_\epsilon(\vec{\rho})$ required by Eq. (7). Details can be found in Ref. 38. Hereafter these correction terms are dropped. Without these terms, the permitted angular momentum coupling is greatly simplified. Equation (8b) now has the simple form

$$(E-\epsilon-K_{\vec{\rho}})G_\epsilon(\vec{\rho})=(\bar{\psi}_\epsilon(\vec{R}),\, V(\vec{\rho})\psi_0(\vec{r})F(\vec{s}))+V(\vec{\rho})G_\epsilon(\vec{\rho})\,. \tag{9}$$

Here we have broken Ψ into its bound and continuum pieces. We reiterate that Eq. (7) implies that solutions of (9) are purely outgoing.

B. Partial wave analysis

To solve coupled Eqs. (8a) and (9), we introduce partial wave expansions of $P\Psi$ and $Q\Psi$,

$$P\Psi(\vec{r},\vec{s})=s^{-1}\sum_{J\mathfrak{M}}F^J(s)\mathcal{Y}_0^{J\mathfrak{M}}(\vec{r},\hat{s})\,, \tag{10a}$$

$$Q\Psi(\vec{R},\vec{\rho})=\rho^{-1}\sum_{J\mathfrak{M}}\sum_{Ll}\int_0^\infty d\epsilon G_{\epsilon Ll}(\rho)\bar{\mathcal{Y}}_{\epsilon Ll}^{J\mathfrak{M}}(\vec{R},\vec{\rho})\,, \tag{10b}$$

where the two parts of Ψ are expressed as sums over terms with definite $J\mathfrak{M}$. The basis functions

$$\bar{\mathcal{Y}}_{\epsilon Ll}^{J\mathfrak{M}}(\vec{R},\hat{\rho})=\{\bar{\psi}_{\epsilon L}(\vec{R}),\, i^l Y_l(\hat{\rho})\}_{J\mathfrak{M}} \tag{11}$$

vector couple the two-body nucleonlike wave functions [see Eq. (3b)] of angular momentum L with relative πN orbital momentum l to form total angular momentum J. The basis function $\mathcal{Y}_0^{J\mathfrak{M}}(\vec{r},\hat{s})$ is used for the special case of a single bound nucleon orbital, for which the subscript zero indicates $\epsilon=\epsilon_0$, $L=0$, and $l=J$. The functions $\bar{\mathcal{Y}}_{\epsilon Ll}^{J\mathfrak{M}}$ (or, separately, the generalized unbarred $\mathcal{Y}_{\epsilon Ll}^{J\mathfrak{M}}$) obey usual orthonormality conditions.

The premultiplications of (5a) and (5b) mentioned above to derive (8a) and (9) now become, respectively, a premultiplication by $\mathcal{Y}_0^{J\mathfrak{M}}(\vec{r},\hat{s})$ with integrations over $\vec{r}$ and $\hat{s}$ or a premultiplication by $\mathcal{Y}_{\epsilon Ll}^{J\mathfrak{M}}(\vec{R},\hat{\rho})$ with integrations over $\vec{R}$ and $\hat{\rho}$. Because $J\mathfrak{M}$ are good quantum numbers of the Hamiltonian $K+U+V$, we arrive at an independent set of coupled equations for each $J\mathfrak{M}$. Members of these sets are

$$[T_r-t_J(s)]F^J(s)=s\int d\vec{r}\int d\hat{s}\,\mathcal{Y}_0^{J\mathfrak{M}}(\vec{r},\hat{s})^* V\mathcal{Y}_0^{J\mathfrak{M}}(\vec{r},\hat{s})s^{-1}F^J(s)+s\sum_{L'l'}\int_0^\infty d\epsilon'\int d\vec{r}\int d\hat{s}\,\mathcal{Y}_0^{J\mathfrak{M}}(\vec{r},\hat{s})^* V\bar{\mathcal{Y}}_{\epsilon' L'l'}^{J\mathfrak{M}}(\vec{R},\hat{\rho})\,\frac{G^J_{\epsilon' L'l'}(\rho)}{\rho} \tag{12a}$$

and

$$[T_r+\epsilon_0-\epsilon-t_l(\rho)]G^J_{\epsilon Ll}(\rho)=\rho\int d\vec{R}\int d\hat{\rho}\,\bar{\mathcal{Y}}_{\epsilon Ll}^{J\mathfrak{M}}(\vec{R},\hat{\rho})^* V\mathcal{Y}_0^{J\mathfrak{M}}(\vec{r},\hat{s})s^{-1}F^J(s)+\rho\sum_{L'l'}\int_0^\infty d\epsilon'\int d\vec{R}\int d\hat{\rho}\,\bar{\mathcal{Y}}_{\epsilon Ll}^{J\mathfrak{M}}(\vec{R},\hat{\rho})^* V\bar{\mathcal{Y}}_{\epsilon' L'l'}^{J\mathfrak{M}}(\vec{R},\hat{\rho})\,\frac{G^J_{\epsilon' L'l'}(\rho)}{\rho}\,, \tag{12b}$$

where $t_{J,l}$ are the partial wave kinetic energy operators, given by

$$t_J(s) = -\frac{\hbar^2}{2m_\pi}\left[\frac{d^2}{ds^2} - \frac{J(J+1)}{s^2}\right] \text{ and } t_l(\rho) = -\frac{\hbar^2}{2\mu}\left[\frac{d^2}{d\rho^2} - \frac{l(l+1)}{\rho^2}\right],$$

and μ is the reduced πN mass. T_π is the pion kinetic energy in the fixed frame, $T_\pi = E - \epsilon_0$, and $\epsilon - \epsilon_0$ is the nucleon excitation energy.

We now introduce an explicit form for the πN interaction. We choose a separable nonlocal interaction in a single partial wave of order l_0 (see Sec. IV A),

$$V(\vec{\rho}, \vec{\rho}') = \frac{4\pi}{2l_0+1} v(\rho)v(\rho') \sum_{m_0} Y_{l_0 m_0}(\hat{\rho}) Y^*_{l_0 m_0}(\hat{\rho}') . \tag{13}$$

Insert (13) into (12a) and (12b). Change integration variables in (12a) from $\vec{r}, \hat{s}$ to $\vec{\rho}, \hat{s}$ (the Jacobian of the transformation is unity), to get

$$[T_\pi - t_J(s)]F^J(s) = \frac{4\pi}{2l_0+1} s\left[W_0^J(s)\frac{F^J(s)}{s} + \sum_{L'}\int_0^\infty d\epsilon' V^J_{0,\epsilon' L' l_0}(s) A^J_{\epsilon' L' l_0}\right] \tag{14a}$$

and

$$[T_\pi + \epsilon_0 - \epsilon - t_l(\rho)]G^J_{\epsilon L l}(s) = \delta_{l,l_0}\frac{4\pi}{2l_0+1}\rho v(\rho)(B^J_{\epsilon L l,0} + A^J_{\epsilon L l}) , \tag{14b}$$

where

$$A^J_{\epsilon L l} = \int_0^\infty d\rho \rho v(\rho) G^J_{\epsilon L l}(\rho) , \tag{15a}$$

$$B^J_{\epsilon L l,0} = \int d\vec{R} \int d\vec{\rho}\, \bar{\mathcal{Y}}^{J\mathfrak{M}}_{\epsilon L l}(\vec{R}, \hat{\rho})^* v(\rho) \mathcal{Y}^{J\mathfrak{M}}_0(\vec{R} - \nu\vec{\rho}, \hat{n}_{\vec{R}+\nu\vec{\rho}}) \frac{F^J(|\vec{R} + \nu\vec{\rho}|)}{|\vec{R} + \nu\vec{\rho}|} , \tag{15b}$$

$$V^J_{0,\epsilon' L' l_0}(s) = \int d\vec{\rho} \int d\hat{s}\, \mathcal{Y}^{J\mathfrak{M}}_0(\vec{s} - \vec{\rho}, \hat{s})^* v(\rho) \bar{\mathcal{Y}}^{J\mathfrak{M}}_{\epsilon' L' l_0}(\vec{s} - \nu\vec{\rho}, \hat{\rho}) , \tag{15c}$$

and

$$W_0^J(s)\frac{F^J(s)}{s} = \sum_{m_0}\int d\vec{\rho} \int d\hat{s}\, \mathcal{Y}^{J\mathfrak{M}}_0(\vec{s} - \vec{\rho}, \hat{s})^* v(\rho) Y_{l_0 m_0}(\hat{\rho}) \int d\vec{\rho}\,' v(\rho') Y^*_{l_0 m_0}(\hat{\rho}') \mathcal{Y}^{J\mathfrak{M}}_0(\vec{R} - \nu\vec{\rho}\,', \hat{n}_{\vec{R}+\nu\vec{\rho}\,'}) \frac{F^J(|\vec{R} + \nu\vec{\rho}\,'|)}{|\vec{R} + \nu\vec{\rho}\,'|} . \tag{15d}$$

In (15d), the $\vec{R}$ dependence that survives after the $\vec{\rho}\,'$ integration must be changed to $\vec{\rho}, \vec{s}$ coordinates, that is, $\vec{R} \to \vec{s} - \nu\vec{\rho}$ after the $\vec{\rho}\,'$ integration. The quantities A and B are numbers—a consequence of the separable πN interaction—while $V^J_{0,\epsilon L l}(s)$ and $W_0^J(s)$ are functions of s. $\hat{n}_{\vec{R}+\nu\vec{\rho}}$ is a unit vector in the $\vec{R} + \nu\vec{\rho}$ direction.

C. Formal solution

First, we solve (14b). Only $l = l_0$ enters and, as noted earlier, there is no homogeneous solution. Therefore

$$G^J_{\epsilon L l_0}(s) = \frac{4\pi}{2l_0+1}(B^J_{\epsilon L l_0,0} + A^J_{\epsilon L l_0})\int d\rho' g_{l_0}(\rho, \rho')\rho' v(\rho') , \tag{16}$$

where $g_{l_0}(\rho, \rho')$ is the outgoing partial wave Green's function. Multiply both sides of (16) by $\rho v(\rho)$ and integrate on ρ. The left-hand side becomes $A^J_{\epsilon L l_0}$, and therefore,

$$A^J_{\epsilon L l_0} = (B^J_{\epsilon L l_0,0} + A^J_{\epsilon L l_0}) I_{l_0}(q) , \tag{17a}$$

where

$$I_{l_0}(q) = \frac{4\pi}{2l_0+1}\int_0^\infty d\rho \rho v(\rho) \int_0^\infty d\rho' g_{l_0}(\rho, \rho')\rho' v(\rho') \tag{17b}$$

and

$$q = [2\mu(E - \epsilon)]^{1/2}/\hbar , \tag{17c}$$

which appears implicitly in the Green's function. I_{l_0} is the same function that appears in the denominator of the free two-body scattering amplitude $t(\vec{\rho}, \vec{\rho}\,')$, see Sec. IV A, Eq. (24). From Eq. (17a),

$$A^J_{\epsilon L l_0} = \mathcal{R}(q) B^J_{\epsilon L l_0,0} , \tag{17a'}$$

where

$$\mathcal{R}(q)=\frac{I_{l_0}(q)}{1-I_{l_0}(q)}\,. \tag{18}$$

The function $\mathcal{R}(q)$ carries the two-body πN resonance into the three-body model. The close relation between $\mathcal{R}(q)$ and the two-body t matrix is seen in Sec. VI B and in the Appendix.

We insert the solution of (14b) into its coupled partner (14a) to get

$$[T_\pi - t_J(s)]F^J(s)=\frac{4\pi}{2l_0+1}s\left[W_0^J(s)\frac{F^J(s)}{s}+\sum_{L'}\int_0^\infty d\epsilon' V^J_{0,\epsilon' L' l_0}(s)\mathcal{R}(q)B^J_{\epsilon' L' l_0,0}\right], \tag{19}$$

where q is related to ϵ' by (17c). The first term on the right-hand side is a local potential that acts on the elastic-channel pion wave function, while the second term is nonlocal (F^J is contained in B^J). The local part contains the nucleon only in its ground state; the nonlocal part contains intermediate propagation of the nucleon in excited states.

The elastic-channel pion scattering equation (19) is difficult to treat, primarily because the numbers $B^J_{\epsilon' L' l_0,0}$ and the functions $V^J_{0\epsilon' L' l_0}(s)$ and $W_0^J(s)$ are not easy to generate. We discuss an approximate generation of these objects in Sec. V. Nonetheless, (19) is a single-particle equation and thus the right-hand side of this equation can be regarded as a microscopically derived, partial wave dependent, complex (from the two-body resonant function $\mathcal{R}$) optical potential acting on $F^J(s)$.

III. PION-NUCLEUS SCATTERING

In this section we generalize the three-body model to describe scattering by a closed shell nucleus. The target nucleus is described as a single determinant of angular momentum zero, composed of shell model orbitals ψ_{aL_0}. To first order in a multiple scattering expansion different target nucleons do not influence each other, therefore the three-body meson-nucleon model can be applied for each nucleon independently.[38] The dynamical equation for the elastic-channel wave function

$$[T_\pi - t_J(s)]F^J(s)=\frac{4\pi}{2l_0+1}s\sum_{aL_0}\left[W^J_{aL_0}(s)\frac{F^J(s)}{s}+\sum_{L_1 L}\int_0^\infty d\epsilon V^J_{a\epsilon}(L_0L_1Ll_0,s)\mathcal{R}(q)B^J_{a\epsilon}(L_0L_1Ll_0)\right]. \tag{20}$$

becomes a sum over contributions from individual ground state orbitals.

The resonance function $\mathcal{R}(q)$ in Eq. (20) is the same quantity obtained in Eq. (18), by solving for the meson-nucleon relative motion in excited states. The angular momentum quantum numbers in Eq. (20) are the following: $J\mathfrak{M}$, the total angular momentum (and its component) of the A nucleons plus pion system (the Hamiltonian conserves $J\mathfrak{M}$ so that the Schrödinger equation decouples in $J\mathfrak{M}$ partial waves); LM, the angular momentum of the one-nucleon excited nucleus; L_1M_1, the angular momentum of the excited nucleon; L_0M_0, the angular momentum of the A-1 unexcited residual nucleus; and lm, the relative πN orbital angular momentum. L_1 and L_0 couple to L, L and l couple to J. These quantum numbers label the generalized coupling potentials

$$\begin{aligned}B^J_{a\epsilon}(L_0L_1Ll_0)=(-i)^{L_1+l_0}i^J(-)^{L_0}\int d\vec{R}\int d\vec{\rho}\sum_{\substack{M_0M_1\\ m_0}}&\bar{\psi}^*_{\epsilon L_1}(\vec{R})Y^*_{L_1M_1}(\hat{R})Y^*_{l_0m_0}(\hat{\rho})\\ &\times v(\rho)\psi_{aL_0}(|\vec{R}-\nu\vec{\rho}\,|)Y^*_{L_0M_0}(\hat{n}_{\vec{R}-\nu\vec{\rho}})Y_{J\mathfrak{M}}(\hat{n}_{\vec{R}+\vec{\nu}\vec{\rho}})\frac{F^J(|\vec{R}+\vec{\nu\rho}|)}{|\vec{R}+\vec{\nu\rho}|}\\ &\times\langle L_0L_1M_0M_1|LM\rangle\langle Ll_0Mm_0|J\mathfrak{M}\rangle\,,\end{aligned} \tag{21a}$$

$$\begin{aligned}V^J_{a\epsilon}(L_0L_1Ll_0,s)=(-i)^{J}i^{L_1+l_0}(-)^{L_0}\int d\vec{\rho}\int d\hat{s}\sum_{\substack{M_0M_1\\ m_0}}&Y^*_{J\mathfrak{M}}(\hat{s})\psi^*_{aL_0}(|\vec{s}-\vec{\rho}\,|)\\ &\times Y_{L_0M_0}(\hat{n}_{\vec{s}-\vec{\rho}})v(\rho)Y_{l_0m_0}(\hat{\rho})\bar{\psi}_{\epsilon L_1}(|\vec{s}-\vec{\nu\rho}\,|)Y_{L_1M_1}(\hat{n}_{\vec{s}-\vec{\nu}\vec{\rho}})\\ &\times\langle L_0L_1M_0M_1|LM\rangle\langle Ll_0Mm_0|J\mathfrak{M}\rangle\,,\end{aligned} \tag{21b}$$

and

$$W^J_{aL_0}(s)\frac{F^J(s)}{s}=\sum_{M_0m_0}\int d\vec{r}\int d\hat{s}\,Y^*_{J\mathfrak{M}}(\hat{s})\psi^*_{aL_0}(r)Y^*_{L_0M_0}(\hat{r})v(\rho)Y_{l_0m_0}(\hat{\rho})$$

$$\times\int d\vec{\rho}\,'v(\rho')Y^*_{l_0m_0}(\hat{\rho}')\psi_{aL_0}(|\vec{R}-\nu\vec{\rho}\,'|)Y_{L_0M_0}(\hat{n}_{\vec{R}-\nu\vec{\rho}\,'})Y_{J\mathfrak{M}}(\hat{n}_{\vec{R}+\vec{\nu\rho}\,'})\frac{F^J(|\vec{R}+\vec{\nu\rho}\,'|)}{|\vec{R}+\vec{\nu\rho}\,'|}\,. \quad (21c)$$

The sum over occupied orbitals in Eq. (20) extends over neutrons and protons and over both spin states. Because the optical potential is degenerate in nucleon spins, the spin sum can be replaced by a multiplicative factor of two. Because pion-nucleon scattering is dominated by isospin $\frac{3}{2}$, the sum over protons and neutrons can also be replaced by a numerical multiplier. For π^+ scattering a neutron orbital simply contributes one-third as much in Eq. (20) as a proton orbital (or conversely for π^- scattering). Hence for ^{16}O we only need to sum explicitly over spatial wave functions and then multiply by $\frac{8}{3}$ to account for the spin and isospin variables.

We note that the continuum energy integral includes by implication a discrete sum over excited bound nucleon orbitals. Equation (20) automatically includes nucleon recoil and the Pauli exclusion principle.

IV. INPUTS FOR THE CALCULATION

In this section we discuss the two potentials—pion-nucleon and nucleon-nucleus—used in our calculations.

A. The pion-nucleon potential

Separable nonlocal interactions are often used in pion-nucleus physics[5,31-33] to represent the strong, isolated pion free nucleon 33-resonance. Under the spin and isospin considerations described at the end of the previous section, we only consider spatial variables, and the πN interaction is taken to have the form

$$V(\vec{\rho},\vec{\rho}\,')=\frac{4\pi}{2l_0+1}v(\rho)v(\rho')\sum_{m_0}Y_{l_0m_0}(\hat{\rho})Y^*_{l_0m_0}(\hat{\rho}')\,. \quad (13)$$

This potential is assumed to act in only the l_0th partial wave. Although the free πN resonance is known to have $l_0=1$, it is convenient to leave (13) in this more general form.

Below we list some familiar two-body results using the separable nonlocal potential (13). The free πN scattering amplitude

$$t=V+V\frac{1}{E-K-V}V=V+V\frac{1}{E-K}t, \quad (22)$$

is given by

$$t(\vec{\rho},\vec{\rho}\,')=\frac{4\pi}{2l_0+1}\frac{v(\rho)v(\rho')}{1-I_{l_0}(q)}\sum_{m_0}Y_{l_0m_0}(\hat{\rho})Y^*_{l_0m_0}(\hat{\rho}')\,, \quad (23)$$

where

$$I_{l_0}(q)=\frac{4\pi}{2l_0+1}\int_0^\infty d\rho\rho v(\rho)\int_0^\infty d\rho' g_{l_0}(\rho,\rho')\rho' v(\rho') \quad (24)$$

and

$$g_{l_0}(\rho,\rho')=-\frac{i}{q}\frac{2\mu}{\hbar^2}\hat{j}_{l_0}(q\rho_<)\hat{h}_{l_0}(q\rho_>) \quad (25)$$

is the partial wave Green's function. Here, μ is the reduced πN mass and q is the wave number in the center-of-mass frame. The function $\hat{j}_{l_0}(\hat{h}_{l_0})$ is a Riccati function, which is a spherical Bessel (Hankel) function times its argument. Resonance behavior is determined by the pole in $1/[1-I_{l_0}(q)]$ in the free scattering amplitude (23).

In momentum space, with the spherical Bessel transform of a potential factor $v(\rho)$ defined by

$$v_{l_0}(k)=\left(\frac{2}{\pi}\right)^{1/2}\int d\rho\rho^2 j_{l_0}(k\rho)v(\rho)\,, \quad (26)$$

we find

$$V(\vec{k},\vec{k}\,')=\frac{4\pi}{2l_0+1}v_{l_0}(k)v_{l_0}(k')\sum_{m_0}Y_{l_0m_0}(\hat{k})Y^*_{l_0m_0}(\hat{k}')\,, \quad (27)$$

$$t(\vec{k},\vec{k}\,')=\frac{4\pi}{2l_0+1}\frac{v_{l_0}(k)v_{l_0}(k')}{1-I_{l_0}(q)}\sum_{m_0}Y_{l_0m_0}(\hat{k})Y^*_{l_0m_0}(\hat{k}')\,, \quad (28)$$

and

$$I_{l_0}(q)=\frac{4\pi}{2l_0+1}\frac{2\mu}{\hbar^2}\int_0^\infty dkk^2\frac{[v_{l_0}(k)]^2}{q^{+2}-k^2}\,, \quad (29)$$

where $q^+=q+i\eta$ expresses the outgoing boundary conditions. $I_{l_0}(q)$ of (24) and $I_{l_0}(q)$ of (29) are identical. The expression for total cross section is given by

$$\sigma_T(q)=\frac{(2\pi)^3}{q}\frac{2\mu}{\hbar^2}\mathrm{Im}\left\{\frac{[v_{l_0}(q)]^2}{1-I_{l_0}(q)}\right\}, \quad (30)$$

where Im takes the imaginary part of what follows.

There is a simple relationship between $[v_{l_0}(q)]^2$ and $\mathrm{Im}I_{l_0}(q)$. Using expression (29) for $I_{l_0}(q)$, we see that the imaginary contribution to $I_{l_0}(q)$ comes only from the pole in the free Green's function $(q^{+2}-k^2)^{-1}$, provided all poles in $v_{l_0}(k)$ are on the imaginary axis. Only the pole at $k=q^+$ contri-

butes to the imaginary part of the integral. The result is

$$\mathrm{Im}I_{l_0}(q) = -\frac{2\pi^2}{2l_0+1}\frac{2\mu}{\hbar^2}q[v_{l_0}(q)]^2 . \tag{31}$$

Insertion of (31) into (30) yields

$$\sigma_T(q) = \frac{4\pi}{q^2}(2l_0+1)\frac{[\mathrm{Im}I_{l_0}(q)]^2}{[1-\mathrm{Re}I_{l_0}(q)]^2+[\mathrm{Im}I_{l_0}(q)]^2} \tag{30'}$$

for the free total cross section. This expression readily generalizes to any number of partial waves and to the inclusion of nucleon spin. We invoke p-wave, $j=\frac{3}{2}$ dominance in the resonance region to specialize to

$$\sigma_T(q) = \frac{8\pi}{q^2}\frac{[\mathrm{Im}I_1(q)]^2}{[1-\mathrm{Re}I_1(q)]^2+[\mathrm{Im}I_1(q)]^2} , \tag{32}$$

or in terms of the phase shift

$$\sigma_T(q) = \frac{8\pi}{q^2}\sin^2\delta_1(q) . \tag{33}$$

By using the experimentally determined phase shifts[52] in (33) and equating to (32), we can determine the range and strength properties of a standard separable nonlocal potential.

B. The fitting procedure

We choose the Yamaguchi form

$$v(\rho) = v_0 e^{-\gamma\rho} , \tag{34}$$

where γ is the inverse range of the interaction and v_0 is its strength. In momentum space this transforms to

$$v_1(q) = 2\left(\frac{2}{\pi}\right)^{1/2}\frac{v_0 q}{(\gamma^2+q^2)^2} . \tag{35}$$

We fit the two parameters in $v(\rho)$ by fixing the energies[52] at which the 33 phase shift takes the two values 90° and 45°. Using relativistic kinematics,[38] we find

$$\gamma = 3.91\ \mathrm{fm}^{-1} \tag{36}$$

$$v_0^2 = -6.26\times10^4\ \mathrm{MeV/fm}^3 . \tag{37}$$

Figure 2 shows the resulting phase shift fit and Fig. 4 shows the fit to the $\pi^+ p$ total cross section.

C. The s-wave mock-up of the p-wave interaction

To simplify the kinematics in the meson optical potential, the calculations in this article are done with an s-wave pion-nucleon interaction [$l_0=0$ in expression (13)], whose form is chosen to fit the p-wave phase shifts.[53] Such an interaction appears complicated in configuration space, because it must produce the effect of the centrifugal potential that governs the actual $l_0=1$ phase shift. However, in momentum space, we see from Eq. (29) that the two Bessel transforms $v_0(k)$ and $v_1(k)$ will produce the same phase shift if they are related by

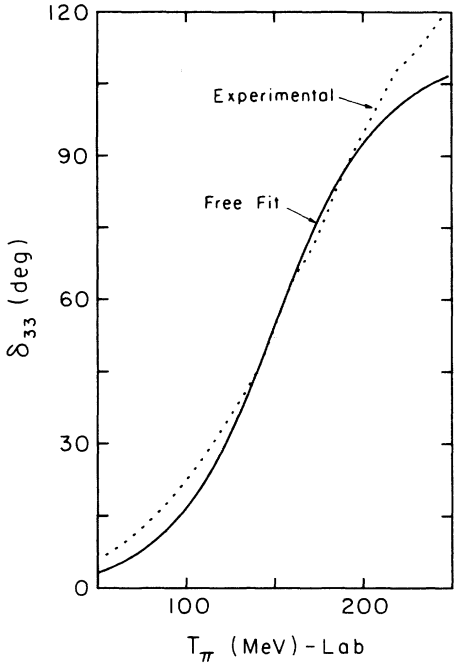

FIG. 2. Comparison of the experimental 33-phase shifts (Ref. 52) with the free fit described in the text.

$$v_0(k) = \frac{1}{\sqrt{3}}v_1(k) . \tag{38}$$

Of course, while such an s-wave interaction reproduces phase shifts, it does not reproduce cross section magnitudes, because the appropriate statistical factor is missing.

D. The binding potential

The binding potential for this study is represented by a central Woods-Saxon well, given by

$$U(r) = \frac{U_0}{1+\exp\left(\frac{r-R}{a}\right)} \tag{39}$$

with typical parameters $U_0=-57$ MeV, $R=r_0A^{1/3}$; $r_0=1.25$ fm, $A=16$, $a=0.5$ fm. This gives bound energy levels at $\epsilon_{1s}=-37.79$ MeV, $\epsilon_{1p}=-22.15$ MeV, $\epsilon_{1d}=-5.97$ MeV, and $\epsilon_{2s}=-5.28$ MeV.

V. CALCULATIONAL DETAILS

A. Approximations

To put the optical potential of Eq. (20) in a usable form, simplified expressions for $B^J_{a\epsilon}(L_0L_1Ll_0)$,

$V^J_{\alpha\epsilon}(L_0L_1Ll_0, s)$, and $W^J_{\alpha L_0}(s)s^{-1}F^J(s)$ [Eqs. (21a)–(21c)] are needed. [The following discussion is also directly applicable to the three-body model, Eqs. (19) and (15b)–(15d).] Calculational difficulties are caused by the mixture of coordinates in the nucleon (and nucleonlike) and pion wave functions.

The use of an s-wave pion-nucleon interaction, with $l_0 = m_0 = 0$, gives the first simplification. The angular momentum (and its magnetic component) of the one-nucleon excited nucleus LM must equal the total angular momentum (and its magnetic component) $J\mathfrak{M}$. Hence the sums over Mm_0 vanish in B, V, and W. Second, the presence of the short ranged $v(\rho)$ factor in B, V, and W suggests dropping the ρ dependence in smooth wave functions, such as the bound nucleon orbitals: $\vec{\rho}$ is dropped in both the radial and angular parts of these wave functions. (A correction to this step is difficult to derive and its effect remains unin-

vestigated.)

Third, we handle the remaining $\vec{\rho}$ dependence in the integrands of $B^J_{\alpha\epsilon}(L_0L_1)$, $V^J_{\alpha\epsilon}(L_0L_1, s)$, and $W^J_{\alpha L_0}(s)s^{-1}F^J(s)$ by approximately factorizing the complicated arguments of the wave functions that appear in these expressions. We follow a method discussed by Nagarajan and Glendenning[54] who exploit the exact factorization of the Born limits of the wave functions (plane waves always factorize!). We demonstrate this method for the pion wave function, for which (up to energy normalization coefficients) the Born correspondence is

$$z^{-1}F^J(z) \to kj_J(kz),$$

where $\vec{z} = \vec{R} + \vec{\nu}\vec{\rho}$. Multiply both sides by

$$\left(\frac{2}{\pi}\right)^{1/2} i^J Y_{J\mathfrak{M}}(\hat{z}) Y^*_{J\mathfrak{M}}(\hat{k})$$

and sum over $J\mathfrak{M}$. This gives

$$\sum_{J\mathfrak{M}} \left(\frac{2}{\pi}\right)^{1/2} i^J z^{-1}F^J(z) Y_{J\mathfrak{M}}(\hat{z}) Y^*_{J\mathfrak{M}}(\hat{k}) \to k \sum_{J\mathfrak{M}} \left(\frac{2}{\pi}\right)^{1/2} i^J j_J(kz) Y_{J\mathfrak{M}}(\hat{z}) Y^*_{J\mathfrak{M}}(\hat{k}),$$

where the right-hand side sums to k times the plane wave with the argument $\vec{k}\cdot\vec{z} = \vec{k}\cdot(\vec{R} + \vec{\nu}\vec{\rho})$. The plane wave readily factorizes. Re-expand each of the exponentials $\exp(i\vec{k}\cdot\vec{R})$ and $\exp(i\vec{k}\cdot\vec{\nu}\vec{\rho})$ and integrate on $\hat{\rho}$. Under this angle integration the wave function becomes

$$\int d\hat{\rho} \sum_{J\mathfrak{M}} \left(\frac{2}{\pi}\right)^{1/2} i^J z^{-1}F^J(z) Y_{J\mathfrak{M}}(\hat{z}) Y^*_{J\mathfrak{M}}(\hat{k}) \to k(2\pi)^{3/2} \sum_{l_1 m_1} \left(\frac{2}{\pi}\right)^{1/2} i^{l_1} j_{l_1}(kR) Y_{l_1 m_1}(\hat{R}) Y^*_{l_1 m_1}(\hat{k})$$
$$\times \sum_{l_2 m_2} \left(\frac{2}{\pi}\right)^{1/2} i^{l_2} j_{l_2}(k\bar{\nu}\rho) Y^*_{l_2 m_2}(\hat{k}) \int d\hat{\rho} Y_{l_2 m_2}(\hat{\rho}). \tag{40a}$$

The $\hat{\rho}$ integral on the right-hand side simplifies the l_2m_2 sums, and the $\hat{k}$ dependence identifies $J\mathfrak{M}$ with l_1m_1 to give

$$\int d\hat{\rho} z^{-1}F^J(z) Y_{J\mathfrak{M}}(\hat{z}) \to 4\pi k j_J(kR) Y_{J\mathfrak{M}}(\hat{R}) j_0(k\bar{\nu}\rho). \tag{40b}$$

The appropriate reversal of the Born limit is to replace $kj_J(kR)$ by $R^{-1}F^J(R)$, so that the angle-averaged factorization results are

$$\int d\hat{\rho} z^{-1}F^J(z) Y_{J\mathfrak{M}}(\hat{z}) \approx 4\pi R^{-1}F^J(R) Y_{J\mathfrak{M}}(\hat{R}) j_0(k\bar{\nu}\rho) \tag{41a}$$

and

$$\int d\hat{\rho} \bar{\psi}_{\epsilon L_1}(z) Y_{L_1 M_1}(\hat{z}) \approx 4\pi \bar{\psi}_{\epsilon L_1}(s) Y_{L_1 M_1}(\hat{s}) j_0(k\bar{\nu}\rho), \tag{41b}$$

where $\vec{z} = \vec{s} - \vec{\nu}\vec{\rho}$ in (41b). The accuracy of this pair of expressions is discussed in the next subsection.

Insertion of the three simplifications of this section—the s-wave interaction, dropping the $\vec{\rho}$ dependence in the bound nucleon orbitals, and factorization—allows the radial ρ integrals and the remaining angle integrals and summations to be done. [The radial ρ integrals are spherical Bessel transforms of $v(\rho)$ as defined by (26) whose wave numbers are explained in the next subsection.] B, V, and W become

$$B^J_{\alpha\epsilon}(L_0L_1) \approx (-i)^{L_1} i^J (-)^{L_0} \left(\frac{\pi}{2}\right)^{1/2} \left(\frac{(2L_0+1)(2L_1+1)}{2J+1}\right)^{1/2} \langle L_0L_100 | J0\rangle \int dR R \bar{\psi}^*_{\epsilon L_1}(R) \psi_{\alpha L_0}(R) F^J(R) v_0(k_\epsilon), \tag{42a}$$

$$V^J_{\alpha\epsilon}(L_0L_1, s) \approx (-i)^J i^{L_1} (-)^{L_0} \left(\frac{\pi}{2}\right)^{1/2} \left(\frac{(2L_0+1)(2L_1+1)}{2J+1}\right)^{1/2} \langle L_0L_100 | J0\rangle \psi^*_{\alpha L_0}(s) \bar{\psi}_{\epsilon L_1}(s) v_0(k_\epsilon), \tag{42b}$$

and

$$sW^J_{aL_0}(s)s^{-1}F^J(s)\approx\frac{\pi}{2}(2L_0+1)[v_0(k_\pi)]^2|\psi_{aL_0}(s)|^2F^J(s), \tag{42c}$$

where factorization is used twice to arrive at (42c).

B. Local WKB

The wave numbers k_π and k_ϵ in expressions (42) arise from the factorization approximations. This procedure extracts $\bar{\nu}$ times the wave number of the factorized wave function, either k_ϵ from $\bar{\psi}_{\epsilon L_1}$ or k_π from F^J, and it uses this wave number in the j_0 function, which, in turn, is folded into $v(\rho)$ to form $v_0(k)$. The local WKB method recognizes that the factorization method is applied independently at each value of the complicated argument z of $\bar{\psi}_{\epsilon L_1}$ or F^J. Therefore, the appropriate wave numbers are determined by the local kinetic energy at each z rather than by the asymptotic kinetic energy. If we omit the ρ part of z in determining the local kinetic energy, the local wave numbers become

$$k_\epsilon(s)=\frac{\bar{\nu}}{\hbar}\{2(m_N+m_\pi)[\epsilon-U(s)]\}^{1/2} \tag{43a}$$

and

$$k_\pi(R)=\frac{\bar{\nu}}{\hbar}[2m_\pi[T_\pi-U^{\rm opt}_{\rm E}(R)]]^{1/2}, \tag{43b}$$

where $U(s)$ is the nucleon binding potential and $U^{\rm opt}_{\rm E}$ is the equivalent local optical potential for the pion. A suitable explicit expression for $U^{\rm opt}_{\rm E}$ is developed in the Appendix.

A numerical check of (41b) for $L_1=0$ not only demonstrates that the local WKB correction to the momenta is essential to give an accurate portrayal of the wave functions but that the accuracy is excellent even for very low energy wave functions. Part of the reason for this is the averaging effect of the angular $\hat{\rho}$ integral in (41).

C. The elastic-channel equation

We now pull the pieces together. The continuum energy integral is broken into a sum over N bins of individual widths $\Delta\epsilon_i$. We define

$$\mathfrak{u}_{aL_0}(s)=2\pi^2(2L_0+1)[v_0(k_\pi(s))]^2|\psi_{aL_0}(s)|^2, \tag{44a}$$

$$\lambda^J_{ai}(L_0L_1)=2\pi^2\Delta\epsilon_i\frac{(2L_0+1)(2L_1+1)}{2J+1}\times\langle L_0L_100|J0\rangle^2\mathfrak{R}(q_{ai}), \tag{44b}$$

where

$$q_{ai}=\frac{1}{\hbar}(2\mu(T_\pi+\epsilon_a-\epsilon_i))^{1/2},$$

$$\tilde{h}_{a\epsilon_i}(L_0L_1,s)=sv_0(k_{\epsilon_i}(s))\psi^*_{aL_0}(s)\bar{\psi}_{\epsilon_iL_1}(s), \tag{44c}$$

$$h_{a\epsilon_i}(L_0L_1,R)=Rv_0(k_\pi(R))\psi^*_{aL_0}(R)\bar{\psi}_{\epsilon_iL_1}(R), \tag{44d}$$

$$P^J_{a\epsilon_i}(L_0L_1)=\int_0^\infty dR h^*_{a\epsilon}(L_0L_1,R)F^J(R), \tag{44e}$$

so that the elastic-channel equation (20) becomes

$$[T_\pi-t_J(s)]F^J(s)=\sum_{aL_0}\left[\mathfrak{u}_{aL_0}(s)F^J(s)+\sum_{L_1}\sum_i^N\lambda^J_{ai}(L_0L_1)\tilde{h}_{a\epsilon_i}(L_0L_1,s)P^J_{a\epsilon_i}(L_0L_1)\right]. \tag{45}$$

Equation (45) is the equation that we solve numerically. The three-body model is also given by (45) but with $aL_0=1s$ only, $L_1=J$ only. Reduction of the optical potential to a more familiar form (the so-called t-rho potential) is presented in the Appendix.

The widths of continuum energy bins used in Eq. (45) are not uniform. Although the resonance function $\mathfrak{R}$ is a rather broad function of ϵ (see Fig. 3), which can be represented by coarse intervals, finer bin widths are necessary to account for the regions of rapid energy dependence of the continuum wave functions $\psi_{\epsilon L_1}$; for example, the $\epsilon\approx4.5$ MeV region of the $L_1=3$ wave function, whose phase shifts show resonance behavior due to the barely unbound $1f$ orbital. Table I gives the bin structure chosen to account for all the ϵ dependent effects.

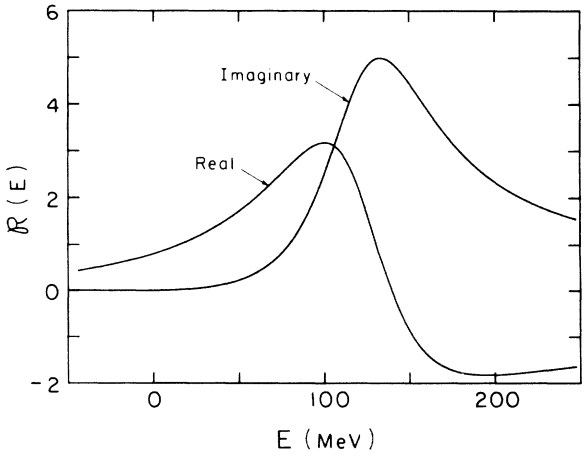

FIG. 3. Real and imaginary parts of the (dimensionless) resonant function $\mathfrak{R}(E)$.

TABLE I. The bin structure used to discretize the nucleonlike continuum, labeled by ϵ. The width $\Delta\epsilon$ of each bin is centered about the corresponding ϵ value.

Bin number	ϵ (MeV)	$\Delta\epsilon$ (MeV)	Bin number	ϵ (MeV)	$\Delta\epsilon$ (MeV)
1	0.1	0.2	13	12	4
2	0.4	0.4	14	16	4
3	1.0	0.8	15	20	4
4	1.8	0.8	16	26	8
5	2.8	1.2	17	35	10
6	3.8	0.8	18	46	12
7	4.3	0.2	19	61	18
8	4.5	0.2	20	85	30
9	4.7	0.2	21	115	30
10	5.2	0.8	22	145	30
11	6.6	2.0	23	175	30
12	8.8	2.4	24	205	30

Scattering through the excited bound nucleon orbitals is not included, because of numerical instabilities. These instabilities are a consequence of the complicated radial form of the pion-nucleon potential for our artificial s-wave interaction, which contains a centrifugal repulsion effect. This problem would not appear in the p-wave calculation, because the meson-nucleon interaction for that case is monotonic and entirely short ranged.

D. Relativistic corrections

We adopt the relativistic Schrödinger equation discussed by Goldberger and Watson.[55] The chief feature of their approach is to use a relativistic kinetic energy operator for the pion projectile, while treating the target nucleons nonrelativistically. Because our calculations are in configuration space, we use semiclassical substitutions to reduce kinetic energy terms that are of higher than second order in the momentum operator.

This procedure is applied to the coupled equations (5a) and (5b) and to the free pion-nucleon scattering analysis that determines the potential parameters. We mention here that our optical equation (45) becomes

$$\left[k_0^2+\frac{d^2}{ds^2}-\frac{J(J+1)}{s^2}\right]F^J(s) = \frac{2(m_\pi c^2+T_\pi)}{\hbar^2c^2}U^{\rm opt}(s,s')F^J(s'), \quad (46)$$

where T_π is the laboratory bombarding energy and

$$k_0^2=(T_\pi^2+2m_\pi c^2T_\pi)/\hbar^2c^2 \quad (47)$$

is the corresponding momentum. $U^{\rm opt}$ is the partially local, partially nonlocal optical potential defined by Eqs. (44), with q_{ai} now given by

$$\hbar^2q_{ai}^2=(\Delta^2-m_\pi^2c^4)\Big/\left(1+\frac{\Delta}{m_Nc^2}\right), \quad (48)$$

where $\Delta=T_\pi+\epsilon_a-\epsilon_i+m_\pi c^2$, and $\Delta/[1+(\Delta/m_Nc^2)]$ is used instead of the reduced mass in the implicit Green's functions. We note that (46) is identical to the Klein-Gordon equation, where the potential is taken to transform as the fourth component of the momentum-energy vector and (as in this procedure) the quadratic term in the potential is dropped.

Besides these modifications to the dynamical differential equations, the kinematics used to derive the optical potential need relativistic corrections. In particular, we replace the mass ratio $\bar{\nu}$ by

$$\bar{\nu}=\frac{m_Nc^2}{E_\pi'+E_N'}, \quad (49)$$

where E_π' and E_N' are the total energies of the pion and nucleon, determined in the πN center-of-mass frame, and k_π defined by Eq. (43b) is relativistically modified, see Sec. VI of Ref. 38, for complete details.

VI. RESULTS AND DISCUSSION

The three-body model expresses the scattering of a pion by a single bound nucleon; when we consider scattering by a nuclear target all the nucleons can affect the meson simultaneously. This leads to very different results for the location of the total cross section maximum. With this warning, we begin this section with a detailed presentation of the results for the three-body calculation. An attempt is made to understand how nucleon binding changes the πN 33-resonance. This is followed by a look at the π-^{16}O results and a discussion of why they differ from the single bound nucleon example. These results and discussions emphasize total cross sections (and their elastic and reaction constituents). We end with a brief presentation of elastic differential cross sections.

A. Three-body model: Results

Here, a pion is scattered by a 1s nucleon bound by 37.8 MeV in a Woods-Saxon well, fitted to the properties of ^{16}O. Figure 4 displays the total cross section for this model, along with the free fit described in Sec. IV. Three changes from the total cross section for a free nucleon are evident: There is an upwards shift of the scattering peak by 40 MeV, there is a reduction of the magnitude, and there is a gentle falloff above the peak energy. We immediately recognize that these effects are not independent. In particular, the reduced cross

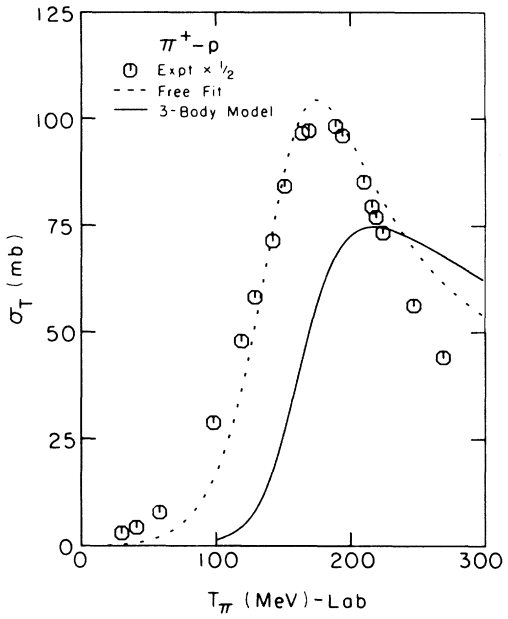

FIG. 4. $\pi^+ p$ cross sections versus pion bombarding energy. The experimental points are halved in magnitude. The free fit is described in Sec. IV. The total cross section for the three-body model is a fit to twelve calculation points, using a cubic interpolation formula.

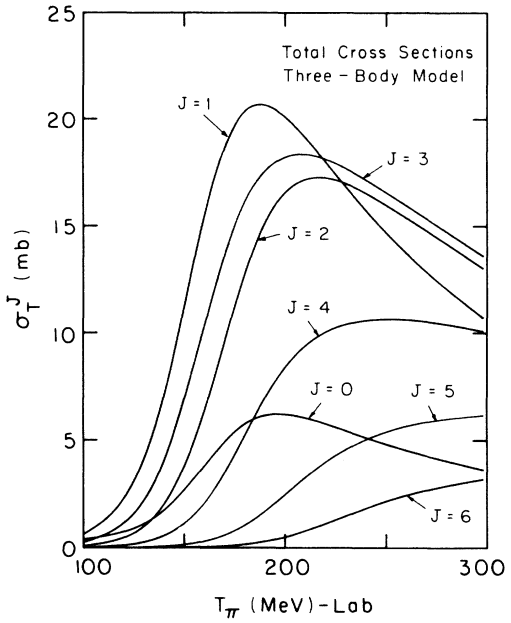

FIG. 5. Contributions of individual partial waves to the three-body model total cross sections.

section magnitude is primarily a consequence of the upwards displacement of the peak, because of the λ^2 coefficient in the theoretical expression. Elastic scattering accounts for about 10% of the total cross section across the resonance region. The lowest partial waves contain most of the elastic contributions. Further discussion of this topic is given with the ^{16}O results, where the elastic behavior is more significant.

Figure 5 gives a breakdown of the total cross section with respect to the angular momentum J in the partial wave expansion of the elastic-channel wave function $F(\tilde{s})$. Although higher partial waves peak at higher bombarding energies, all waves, even the strong $J=1$ wave, peak above the free resonance energy. The $J=3$ cross section is unusually strong. This effect is explained by the next series of figures.

Detailed information about the dynamics of our model is obtained by examination of the reaction cross section,[56]

$$\sigma_R^J = -\frac{2(m_\tau + T_\tau)}{\hbar^2 k^3} 4\pi(2J+1) \sum_i^N \mathrm{Im}\{\lambda_i P_i \tilde{P}_i^*\} . \quad (50)$$

This cross section is expressed in terms of quantities defined by Eqs. (44), with the bin index i indicating all relevant subscripts on λ_i and P_i; $\tilde{P}_i$ is defined by (44e), with $\tilde{h}_i$ instead of h_i. Because $P_i \tilde{P}_i^*$ is nearly real and positive, different ranges of ϵ contribute almost independently in Eq. (50). This property enables us to identify the summand of Eq. (50) as an approximate *differential reaction cross section* $d\sigma_R^J/d\epsilon$ that indicates through which intermediate nuclear states the reaction proceeds. Figures 6–8 are graphs of the

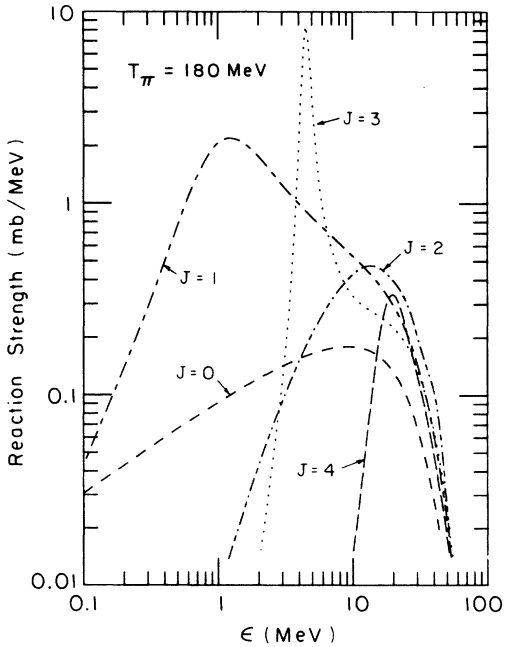

FIG. 6. Contributions of individual partial waves to the reaction strength $d\sigma_R^J/d\epsilon$ for the three-body model at T_τ = 180 MeV. There is a cubic interpolative fit to the twenty-four ϵ bins.

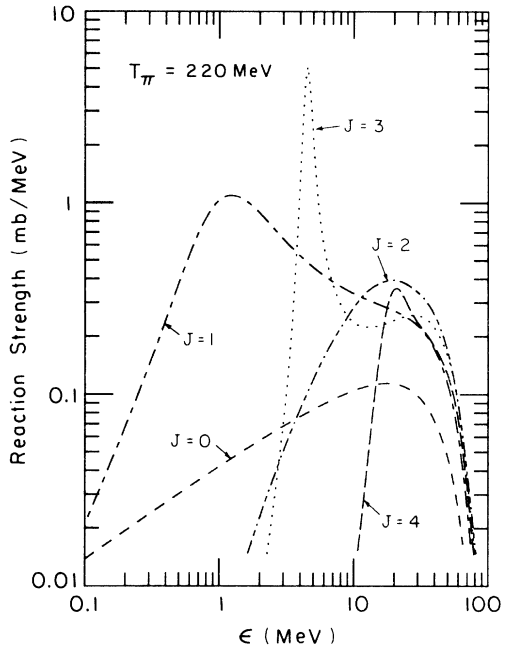

FIG. 7. Same as Fig. 6, $T_\pi = 220$ MeV.

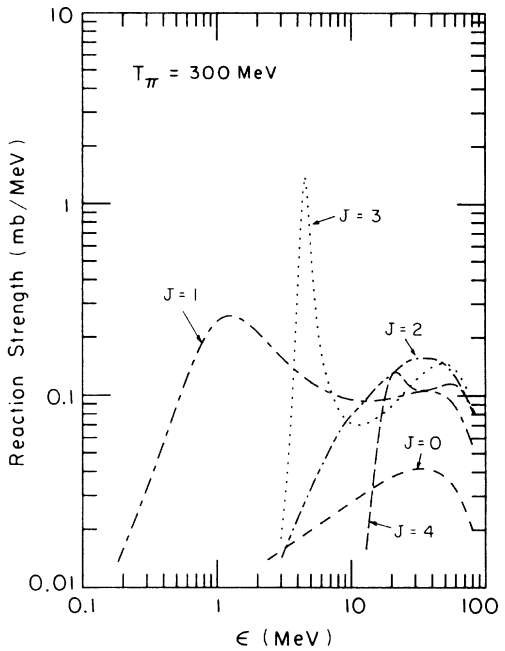

FIG. 8. Same as Fig. 6, $T_\pi = 300$ MeV.

approximate $d\sigma_R^J/d\epsilon$.

The $J=1$ and 3 peaks at 1 and 4.5 MeV in Figs. 6–8 reflect the structure of the low lying nucleon spectrum. These peaks arise from the barely unbound $2p$, $1f$ states of the Woods-Saxon binding potential. However, the humps or plateaus in all partial waves at higher ϵ are caused by the pion-nucleon resonance. Contributions to the reaction cross section from low energy ($\epsilon < 10$ MeV) and high energy ($\epsilon > 10$ MeV) nucleon excitations are obscured by the logarithmic energy scale in Figs. 6–8, therefore they are summarized in Table II. Except at low pion energies, most of the contributions at low nucleon energies come from the $1f$, $2p$ spikes.

Figures 6–8 and Table II show that meson scattering receives significant contributions both from low excitation energies that are influenced by nuclear structure effects and from higher energies that correspond to free nucleon recoil. The importance of structure effects suggests significant corrections to an impulse approximation approach, in which free nucleon recoil is regarded as dominant.

B. Three-body model: Discussion

The energy dependence of the total cross section for the three-body model is obtained by solving the elastic-channel Schrödinger equation (45) for a single bound target nucleon. Equation (45) takes the reduced form

$$[T_\pi - t_J(s)]F^J(s) = 2\pi^2\Big[v_0(k_\pi(s))^2\,|\psi_0(s)|^2F^J(s) + \int d\epsilon v_0(k_\epsilon(s))\mathcal{R}(T_\pi+\epsilon_0-\epsilon)s\psi_0^*(s)\bar{\psi}_{\epsilon J}(s)\int dR v_0(k_\pi(R))R\psi_0(R)\bar{\psi}^*_{\epsilon J}(R)F^J(R)\Big]. \quad (51)$$

TABLE II. Partial reaction cross sections (mb) for the three-body model are tabulated by low ($\epsilon < 10$ MeV) versus high ($\epsilon > 10$ MeV) excited nucleon contributions. The numbers presented are integrals of the $d\sigma_R/d\epsilon$ curves shown, for example, in Figs. 6–8 over the appropriate ϵ regions. T_π is the laboratory pion bombarding energy (MeV).

T_π	100	120	140	160	180	190	200	220	250	300
$\sigma_R(\epsilon<10)$	0.6	2.6	8.8	19	23	21	18	13	8	3.5
$\sigma_R(\epsilon>10)$	0.2	1.0	4.4	15	33	42	49	56	58	54
$\frac{\sigma_R(\epsilon<10)}{\sigma_R}$	78%	73%	67%	57%	41%	33%	27%	19%	11%	6%

The results of Sec. VI A were obtained from this equation. The energy dependence in Eq. (51) not only enters through the parameters T_π on the left-hand side (LHS), it also occurs in the resonance function $\mathcal{R}$ and in the local momenta of the interaction matrix elements $v_0(k_\epsilon(s))$ and $v_0(k_\pi(R))$. The function $\mathcal{R}$ has a simple pole structure, which we recall from Eq. (18) as

$$1+\mathcal{R}(E)=\frac{1}{1-I(E)}\,, \tag{52}$$

with a consequent strong peak in $\mathcal{R}(E)$ at $E_{\text{peak}}=139$ MeV, as seen in Fig. 3. [The quantity $I(E)$ is defined in Eq. (24).] Evidently $\mathcal{R}(E)$ in Eq. (51) has the argument

$$E=T_\pi+\epsilon_0-\epsilon\,. \tag{53}$$

The $1+\mathcal{R}(E)$ form of Eq. (52) tends to appear approximately on the right-hand side of Eq. (51), when the two terms of that expression are combined.

Discussions of expressions like Eq. (51) are usually based on approximate comparisons with related expressions for free pion-nucleon scattering. The free nucleon limit of Eq. (51) is obtained in the Appendix as

$$[T_\pi-t_f(s)]F_f^J(s)=2\pi^2 t_f(T_\pi-\epsilon_\pi;k_\pi,k_\pi)\,|\psi_0(s)|^2F_f^J(s)\,. \tag{54}$$

In this limit the nuclear ground state wave function $\psi_0(s)$ has small amplitude and very long range. The arguments in t_f are center-of-mass quantities; in particular, ϵ_π is the nucleon energy at which the momentum of the excited nucleon matches that of the pion, therefore $T_\pi-\epsilon_\pi$ is the collision energy in the center-of-mass system. The amplitude t_f does not contain any projection operators that restrict its effect to particular partial waves, therefore the long range of the effective optical potential in Eq. (54), determined by $\psi_0(s)$, implies that many partial waves contribute to laboratory frame meson scattering. And because the free optical potential is very smooth, the energy dependence of σ is dominated by that of

$$t_f(T_\pi^{\text{c.m.}};k_\pi,k_\pi)=\frac{v(k_\pi)v(k_\pi)}{1-I(T_\pi^{\text{c.m.}})}\,. \tag{55}$$

In turn, the energy dependence of t_f is dominated by the denominator of (55), and it peaks at $T_\pi^{\text{c.m.}}=139$ MeV. The corresponding free nucleon peak in the laboratory system is at $T_\pi=176$ MeV.

The exact amplitude t_f of the free nucleon limit has the same $1+\mathcal{R}(E)$ structure that emerges approximately in the right-hand side of Eq. (51). It is therefore of interest to discuss Eq. (51) by replacing the right-hand side of that equation by the expression of Eq. (54), but with t_f substituted by a "bound t amplitude" t_b derived from t_f by a suitable alteration of the energy variable.

In the exact equation (51) the argument of $\mathcal{R}(E)$ contains the excitation energy variable ϵ. A plausible t_b is obtained by replacing this ϵ by an average $\bar{\epsilon}$, so that the energy argument of t_b becomes

$$T_\pi+\epsilon_0-\bar{\epsilon}\,.$$

In our three-body model $\epsilon_0=-38$ MeV and $\bar{\epsilon}$ is positive. We therefore expect the peak of t_b to occur at a larger value of T_π than in the free nucleon case, in agreement with the accurate solution of Eq. (51). More quantitatively, the energy argument in t_f is $T_\pi-\epsilon_\pi$, where ϵ_π is the recoil energy discussed previously. Therefore the energy shift between the arguments of t_f and t_b must be

$$\epsilon_\pi-\epsilon_0+\bar{\epsilon}\,.$$

In the vincinity of the resonance, this estimate for the upwards shift of the peak becomes $(37-38+25)$ MeV, and it predicts a cross section maximum at $T_\pi\approx 202$ MeV. In this estimate we use $\bar{\epsilon}\approx 25$ MeV, derived as the median excitation energy for contributions to the reaction cross section in the resonance region.

The energy dependence of the elastic-channel wave function $F^J(s)$ is also influenced by the interaction matrix elements $v_0(k_\epsilon(s))$ and $v_0(k_\pi(R))$. Because these matrix elements tend to be proportional to the arguments k_ϵ and k_π, which are WKB local momenta in the wave functions $\bar{\psi}_\epsilon(\vec{R})$ and $F(\vec{s})$, respectively, the matrix elements must be sensitive to effects that influence those wave functions. In the three-body model we are especially concerned with $v_0(k_\epsilon(s))$, because the magnitude of $k_\epsilon(s)$ in the nuclear interior is increased by the binding potential that determines $\bar{\psi}_\epsilon(\vec{R})$. This effect greatly increases the effective strength of $v_0(k_\epsilon(s))$ at small ϵ, and it therefore enhances the role of low ϵ in our calculation. Larger values of the median excitation energy $\bar{\epsilon}$ would have been obtained in the absence of this local momentum effect.

Thus the influence of the binding potential on the excited states $\psi_\epsilon(\vec{R})$ tends to reduce the upshift of the cross section peak. This seems to be related to the cancellation of the potential in perturbative investigations[33,37] of t_b.

Because local WKB is an effect of the nuclear interior, it should be less important in the ^{16}O calculation, where the cooperation of all the target nucleons leads to strong absorption and reduces scattering from the nuclear interior. On the other hand, the absorptive effect for ^{16}O may be counterbalanced by the increased shift of the local mo-

mentum in the $v_0(k_\pi(s))$ matrix element, caused by the stronger meson optical potential. Thies[57] has noted the dependence of binding corrections on nuclear density.

Centrifugal repulsion also suppresses the nuclear interior, therefore we expect the effect of local WKB to be less important for higher partial waves. It is interesting to see in Figs. 6–8 how the reaction strength peaks at higher ϵ values as J increases, gradually approaching the asymptotic momentum matching value ϵ_π. This contributes to the effect (Fig. 5) that total cross sections for higher partial waves peak at progressively higher bombarding energies.

Naturally, the cross section for higher partial waves is also displaced upwards in energy because of elementary centrifugal barrier effects in the elastic channel. This is an indirect consequence of the binding potential, in the sense that binding has caused the target nucleon to be spatially localized.

In summary, the peak cross section for our three-body model is substantially shifted upwards in energy. Although in disagreement with some other recent work,[33,34] this result does resemble that of Wakamatsu[15] and that of Amado, Lenz, and Yazaki in their peripheral study of the impulse approximation.[36] Our upwards shift is caused by the localization of the target nucleons and by the greater influence of the binding potential in the $\psi_0(r)$ ground state than in the $\bar{\psi}_\epsilon(R)$ excited states. It is interesting that in the *nuclear matter limit of our model*, the effects of binding tend to cancel out of the calculation.[58] Perturbative methods used by other authors may imitate this cancellation.

Further interpretations of the results can be based on a local equivalent of the optical potential in Eq. (51), the so-called "trivially equivalent local potential" of Perey and Buck,[59] defined by

$$\tilde{U}^J(s) = \frac{\int dr U^J_{\rm opt}(s,R) F^J(R)}{F^J(s)}, \qquad (56)$$

where $U^J_{\rm opt}$ includes both the local and nonlocal parts of the optical potential on the right-hand side of Eq. (51). This trivial local potential tends to have poles, because the nonlocal potential in the numerator allows the zeros of the numerator to be displaced from those of the denominator. From the widths of these poles we estimate that the meson optical potential has a range of nonlocality of about $\frac{1}{2}$ fm. We also find that the overall range of the trivial local potential is nearly the same as that of the nuclear density, despite the presence of continuum intermediate states, which extend to large radii. Such trivial local potentials were computed[38] for the three-body case and for the π-^{16}O case. Figs. 9(a) and 9(b) are typical examples.

C. π-^{16}O: Results

The optical potential for ^{16}O is a sum of contributions from the interactions of the meson with individual target nucleons, as is typical of first-order multiple scattering theory. However, the scattering caused by this optical potential is a nonlinear consequence of its constituent parts, therefore important new effects must appear.

In Fig. 10 we see that the peak of the total cross section for the ^{16}O target is shifted some 53 MeV below the single bound nucleon result; the peak is even 13 MeV below the free resonance position. Thus although binding causes an upwards shift of the peak in the cross section, the presence of

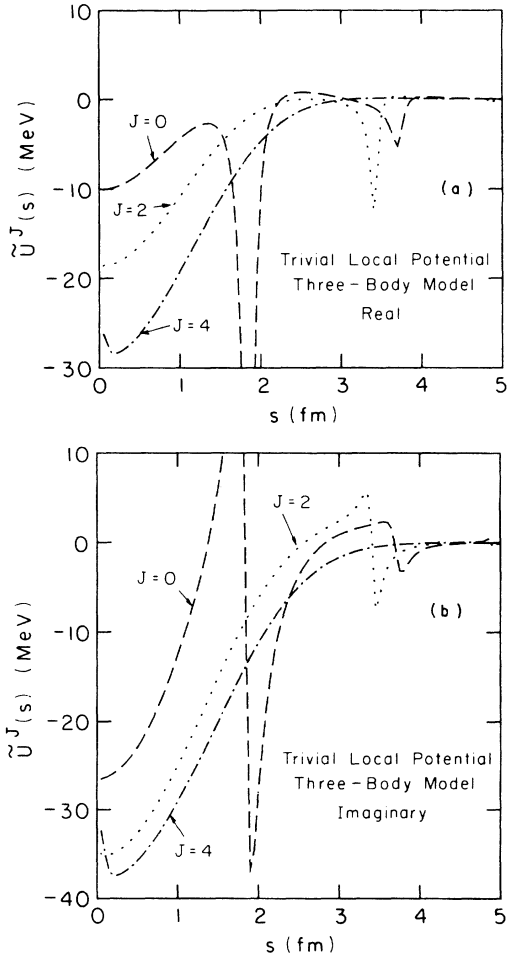

FIG. 9. (a) The real part of the trivially equivalent local optical potential for even partial waves and 220 MeV bombarding energy, as given by Eq. (56), three-body model. (b) Same as (a), except the imaginary part.

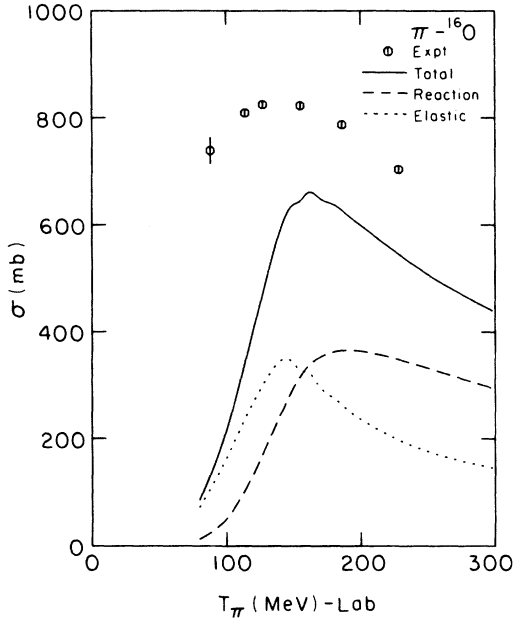

FIG. 10. Total, reaction, and integrated elastic cross sections for π-^{16}O, derived by cubic interpolation to sixteen calculation points. Experimental points (Ref. 62) are computed by $\frac{1}{2}(\sigma_{\pi^+} + \sigma_{\pi^-})$.

many bound nucleons in the form of a nucleus overwhelms the upshift. We address this difference in subsection D.

The principal new effect in Fig. 10 is that elastic scattering plays a major role, unlike in the three-body results. The elastic and reaction maxima straddle the peak of the total cross section, about 50 MeV apart. The total cross section still shows a gentle falloff above resonance, an effect attributed to the reaction cross section.

Figures 11 and 12 give partial wave breakdowns for the calculated elastic and reaction cross sections. We notice that elastic cross sections emphasize lower partial waves than reaction cross

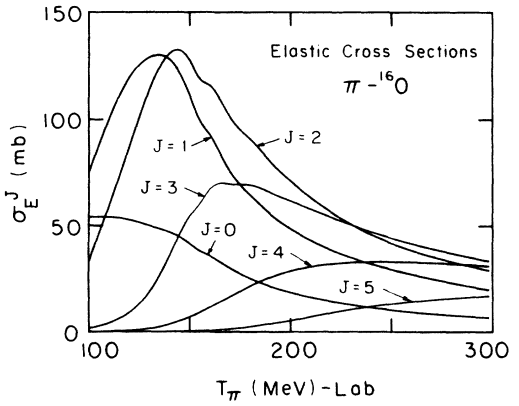

FIG. 11. Contributions of individual partial waves to the calculated elastic cross section, π-^{16}O.

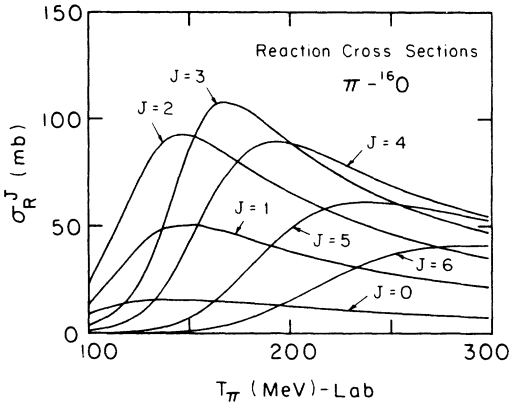

FIG. 12. Contributions of individual partial waves to the calculated reaction cross section, π-^{16}O.

sections. As in the three-body model, higher partial waves peak at higher energies and have smoother high energy falloffs. However the occupied $1p$ nucleon orbital introduces a unit of angular momentum that destroys the previous one-to-one correspondence between J and the angular momentum of the excited nucleon, therefore the partial wave breakdowns are less sensitive to the nuclear structure of the $2p$, $1f$ shell.

The dependence of reaction strength on the excitation energy ϵ was investigated, as in the calculations that led to Figs. 6–8 for the three-body case. Here again the angular momentum of the occupied $1p$ orbital complicates the interpretation, as with the cross sections. We show Fig. 13 as an example[38] of the dependence of the reaction strength on ϵ. Table III summarizes the relative importance of the low energy (<10 MeV) versus high energy (>10 MeV) regions of excitation.

D. π-^{16}O: Discussion

Despite the increased elastic cross section, the *reaction cross section* still is the largest part of the ^{16}O scattering. It remains subject to the considerations discussed in subsection B for the three-body model. Once again we expect the location of the peak to be displaced upwards by a binding correction to the energy argument in the resonance function $\mathcal{R}(E)$. However, the average binding energy that enters this shift must be determined by both the $1s$ and $1p$ orbitals in ^{16}O, giving $\frac{1}{4}(\epsilon_{1s} + 3\epsilon_{1p}) = 26$ MeV, instead of the previous 38 MeV. Thus the upward shift due to binding is less than in the three-body model.

There is an important downward shift of the reaction cross section, which occurs because throughout the broad energy region affected by the resonance the few partial waves that interact with the target nucleus are totally absorbed. In this

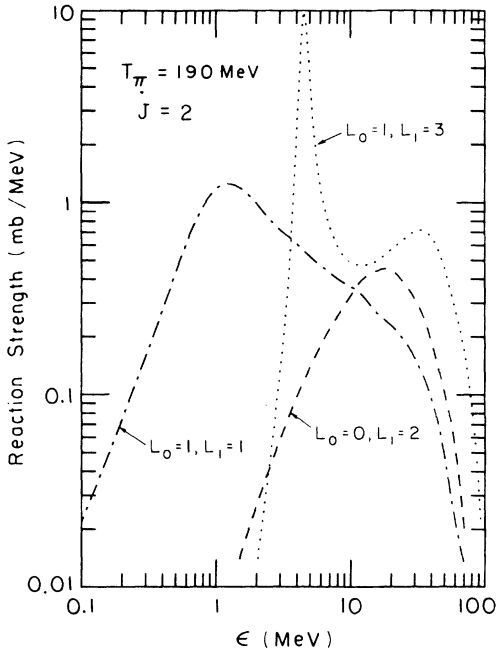

FIG. 13. Contributions of the possible nucleon couplings to the reaction strength $d\sigma_R(L_0,L_1,J)/d\epsilon$ for $\pi^-{}^{16}$O at T_π = 190 MeV, J = 2. Here $J=|\vec{L}_0+\vec{L}_1|$, L_0 and L_1 are the ground state and excited nucleon angular momenta, respectively.

"plateau" region the reaction cross section is determined by the meson wavelength and the nuclear radius, and it becomes

$$\sigma_R=\pi\lambda^2\sum_{J=0}^{kR}(2J+1)\simeq\pi(R+\lambda)^2.$$

The presence of λ causes this black disk cross section to be larger at the low energy end of the plateau.[60,1b]

Different considerations apply to the *elastic cross section* for $\pi^-{}^{16}$O scattering. We may ask first, why is elastic scattering now comparable in magnitude to reaction scattering? Second, why does elastic scattering peak 50 MeV below the maximum of the reaction cross section? And third, why does elastic scattering exhibit a sharp falloff above resonance?

(i) The enhanced importance of elastic scattering is immediately a consequence of the nonlinear relation between the optical potential and the cross section. The optical potential for ^{16}O is approximately 11-fold stronger than for a single nucleon (for a π^+ projectile we get 8 from the protons and $\frac{8}{3}$ from the neutrons). This strengthening of the already strong absorptive part of the optical potential increases the nearly saturated reaction cross section by only a factor of about 5. However, the associated elastic cross section for a single nucleon is very small, so it is understandable that the increase for ^{16}O is nearly the Born ratio,

$$\frac{\sigma_E(^{16}\mathrm{O})}{\sigma_E(p)}\approx\left|\frac{U_{\mathrm{opt}}(^{16}\mathrm{O})}{U_{\mathrm{opt}}(p)}\right|^2\approx 10^2.$$

What was a few millibarns (σ_E) out of seventy millibarns (σ_T) for the single bound nucleon target, is now half of several hundred millibarns for the ^{16}O target.

(ii) The lower energy peak in the elastic cross section is associated with a maximum of the real part of the optical potential at that energy. This energy is well below the region of maximum strength of the imaginary optical potential, therefore strong absorption does not mask the role of the real potential. There are two real terms in the optical potential. While the local term is a real, slowly varying, always attractive, function of pion energy, the real part of the nonlocal term varies sharply with energy, roughly as $\mathrm{Re}\mathfrak{R}(E)$. As we see in Fig. 3, $\mathrm{Re}\mathfrak{R}(E)$ resembles the derivative of $\mathrm{Im}\mathfrak{R}(E)$ and so changes from attractive to repulsive as E goes through resonance. The largest values of $\mathrm{Re}\mathfrak{R}(E)$ are displaced from the peak of $\mathrm{Im}\mathfrak{R}(E)$ by approximately the half width of the resonance, the 50 MeV gap between the elastic and reaction peaks reflected in Fig. 10. We note finally that the attractive peak of $\mathrm{Re}\mathfrak{R}(E)$ at low energy is in phase with the local potential, but the repulsive peak at high energy is largely canceled by the local potential.

TABLE III. Partial reaction cross sections (mb) for $\pi^-{}^{16}$O are tabulated by low ($\epsilon<10$ MeV) versus high ($\epsilon>10$ MeV) excited nucleon contributions. The numbers presented are the integrals of the $d\sigma_R/d\epsilon$ curves shown, for example, in Fig. 13 over the appropriate ϵ regions. T_π is the laboratory pion bombarding energy (MeV).

T_π	80	100	120	140	160	170	180	190	220	300
$\sigma_R(\epsilon<10)$	10	33	72	106	111	99	82	66	35	12
$\sigma_R(\epsilon>10)$	3	18	62	138	223	255	281	300	319	280
$\frac{\sigma_R(\epsilon<10)}{\sigma_R}$	75%	65%	54%	43%	33%	28%	23%	18%	10%	4%

(iii) The rapid decrease of the elastic cross section at high bombarding energies is probably related to the interference mentioned above, between the attractive local part of the real optical potential and the repulsive part of the nonlocal real potential at high T_π. Graphs of the trivial local potential for the ^{16}O case show the consequent reversal of the sign of the real optical potential as the bombarding energy passes through the resonance region.[38] Sedlak and Friedman[61] attribute some of the downward displacement of the cross section peak to this reversal of the real potential, using the argument that the attractive potential below resonance enhances the absorptive cross section in that region of energy.

Another physical effect produced by the attractive real part of the optical potential at low bombarding energies is an increase of the meson kinetic energy in the nuclear interior. This must contribute to the downwards displacement of the cross section peak.

E. Differential cross sections

Figure 14 displays elastic differential cross sections for π^--^{16}O scattering, along with experimental data points. The qualitative agreement between theory and experiment, in spite of our use of an $l=0$ pion-nucleon interaction, should probably be attributed to the essentially diffractive scattering of mesons by ^{16}O.

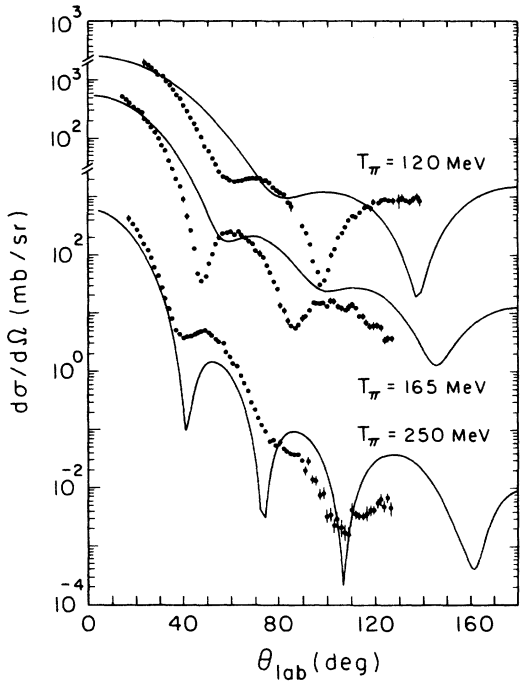

FIG. 14. Calculated differential elastic cross sections for π^--^{16}O at $T_\pi = 120$, 165, and 250 MeV. Data points (Ref. 63) for π^+-^{16}O at $T_\pi = 114$, 163, and 240 MeV (π^--^{16}O not significantly different). All quantities are in the laboratory frame.

VII. CONCLUSIONS

One result of this study is the derivation of a parameter free pion-nucleus optical potential. It contains local and nonlocal aspects. The local term is real, it refers to a struck nucleon that remains in its original occupied orbital. The nonlocal term is complex and partial wave dependent, it describes the intermediate excitation of the struck nucleon into the continuum. The overall range of the potential is roughly that of the nuclear single-particle density, the nonlocality is of the order of $\frac{1}{2}$ fm. The pion and nucleon momenta in the optical potential are determined locally by the WKB method described in Sec. V B.

Our investigation with this optical potential shows that scattering of a pion by a *single bound nucleon* causes an upwards shift of the peak cross section by about the amount of binding. Much of this effect can be attributed to a simple change in the available system energy. However, binding also affects the cross section through the interaction matrix elements, and these are influenced in a sensitive fashion by the local momentum of the intermediate nucleon. This effect tends to oppose the binding energy shift, however, it is much weaker.

The complicated spectrum of intermediate states that contribute to the "bound t amplitude" t_b in our three-body calculation suggests that impulse approximations can be very misleading. Important contributions to t_b are obtained not only at the large nucleon energies ϵ produced by recoil from the incident meson, but also at low ϵ values, where there are resonances that affect particular partial waves. Although less explicit analyses do not encounter our low ϵ effects, we note that the angle dependent intermediate state energies in some recent momentum space approximations[30,32,33,35-37] for t_b would correspond in our approach to the presence of a large range of ϵ values.

When *several bound nucleons are combined* to form a nucleus, the maximum of the total cross section is at a lower energy than the peak of the free 33-resonance. This down shift, within the rather broad width of the 33-resonance, is caused by nonlinearities in the simultaneous scattering of one meson by several target nucleons. For example the saturated absorptive effect of the optical potential gives rise to a plateau tilting χ^2 correction in the reaction cross section. But the main difference is caused by the real part of the

optical potential. The very fact that the real potential is weak in the three-body model means that its importance relative to the imaginary potential tends to be enhanced by the number of nucleons that are present in a many-nucleon target.

The strength of the nonlocal real part of the optical potential is concentrated away from the absorptive peak, in the wings of the 33-resonance region, and it changes from attractive to repulsive as the bombarding energy passes through the free resonance. Hence, the nonlocal real part and the smooth local real part of the optical potential interfere constructively below the free resonant energy and they interfere destructively above resonance. This causes a large downwards shift of the cross section maximum.

The conclusions discussed above should not depend strongly on the special assumptions of our analysis. Rather, they are primarily determined by nuclear structure or strong absorption, and by the great width of the πN resonance. Careful introduction of local momentum values is also necessary. However, although the artificial $l=0$ πN interaction in our preliminary calculation probably does not produce misleading total cross sections, further work with a more physical $l=1$ interaction is in progress. The $l=1$ interaction has a more reliable short ranged behavior in configuration space, and this will allow the inclusion of bound intermediate states $\bar{\psi}_\epsilon$ that are omitted from the present calculation. The accuracy of the more basic approximations introduced in Sec. II is difficult to assess, despite numerical tests.[38] However, these approximations are all based on the short range of the πN interaction, perturbation expansions are avoided. It was already pointed out in Sec. VI that our avoidance of perturbation methods is a considerable departure from previous work.

ACKNOWLEDGMENTS

This study was begun at the University of Washington where N. A. spent a sabbatical year as a visiting professor and M. S. was a visiting graduate student. We are grateful for the hospitality of the U. W. Physics Department and for useful discussions with G. A. Miller and E. M. Henley. N. A. acknowledges a discussion about three-body models with A. W. Thomas. We are grateful to C. Schmit for copies of articles by the Orsay group and a copy of his unpublished thesis. E. R. Siciliano graciously provided some unpublished scattering calculations. Discussions with M. B. Johnson, F. Tabakin, and C. M. Vincent are also gratefully acknowledged. The hospitality of Dr. L. Rosen and the Los Alamos Meson Physics Facility enabled several of these discussions to take place. We thank D. M. Butler for his invaluable assistance in preparation of the figures. Research support was provided by the National Science Foundation.

APPENDIX: OPTICAL POTENTIAL LIMITS

In this appendix we consider two limits of the optical potential of Eq. (45). Both these limits—the closure limit and the free binding limit—coalesce the local and nonlocal aspects of the optical potential into a single local term. The closure approximation reduces the optical potential in (45) to the "t-rho" form, which can be obtained by an impulse approximation approach; the free limit of (45) is a special case of the t-rho potential with a specific closure energy.

In the closure approximation the ϵ parameter in Eq. (45) is replaced by a constant, interpreted as an average nucleon excitation energy, then the intermediate nuclear states are summed. The energy variable ϵ appears in Eq. (45) in $\mathcal{R}(T_\pi+\epsilon_a-\epsilon)$ and in $v_0(k_\epsilon(s))$, besides the nucleon wave functions $\bar{\psi}_{\epsilon L_1}$. We replace $T_\pi+\epsilon_a-\epsilon$, by $T_\pi-\bar{\epsilon}$ and k_ϵ by k_π. Completeness,

$$\sum\!\!\!\!\!\!\int d\epsilon\,\bar{\psi}_{\epsilon L_1}(s)\bar{\psi}^*_{\epsilon L_1}(R)=\frac{\delta(s-R)}{s^2}\,, \tag{A1}$$

where we extend the sum to include the occupied orbitals, reduces the optical potential in (45) to

$$U^{\rm opt}(s)=\sum_{aL_0}2\pi^2(2L_0+1)v_0(k_\pi)\times\left[1+\sum_{L_1}\frac{2L_1+1}{2J+1}\langle L_0L_100|J0\rangle^2\times\mathcal{R}(T_\pi-\bar{\epsilon})v_0(k_\pi)|\psi_{aL_0}(s)|^2\right], \tag{A2}$$

where, for simplicity, we drop the local momentum $k_\pi(s)$ in favor of the asymptotic k_π. The L_1 sum over the parity Clebsch-Gordan coefficients is a special case of the completeness condition,

$$\sum_{L_1}\frac{2L_1+1}{2J+1}\langle L_0L_100|J0\rangle^2=\sum_{L_1}\langle JL_000|L_10\rangle^2=1\,.$$

Definition (18) for $\mathcal{R}$ can be written as

$$1+\mathcal{R}(T_\pi-\bar{\epsilon})=\frac{1}{1-I_0(T_\pi-\bar{\epsilon})}\,, \tag{A3}$$

where I_0 is defined by Eq. (24). The t amplitude for the s-wave πN interaction, see Eq. (28), is

$$t(T_\pi-\bar{\epsilon};k_\pi,k_\pi)=\frac{v_0(k_\pi)v_0(k_\pi)}{1-I_0(T_\pi-\bar{\epsilon})}\,, \tag{A4}$$

so that (A2) is

$$U^{\rm opt}(s)=2\pi^2 t(T_\pi-\bar{\epsilon};k_\pi,k_\pi)\sum_{aL_0}(2L_0+1)\left|\psi_{aL_0}(s)\right|^2. \tag{A5}$$

The sum over a extends over neutrons and protons and over both spin states. These are replaced by the numerical multiplier $(4/A)(Z+N/3)$, where Z is the number of protons and here N is the number of neutrons. The sum for doubly closed shell nuclei is thus restricted to spatial wave functions only. The nuclear single-particle density is identified as

$$\rho_{\rm Nucl}(s)=\frac{4}{A}\sum_{aL_0}(2L_0+1)\left|\psi_{aL_0}(s)\right|^2, \tag{A6}$$

with normalization $\int_0^\infty ds\, s^2\rho_{\rm Nucl}(s)=1$, so that (A5) becomes

$$U^{\rm opt}(s)=2\pi^2\left(Z+\frac{N}{3}\right)t(T_\pi-\bar{\epsilon};k_\pi,k_\pi)\rho_{\rm Nucl}(s). \tag{A7}$$

This expression is consistent with usual momentum space approaches.

The above approximate local potential is applied in Sec. V for the calculation of the local momentum $k_\pi(s)$ by using a real equivalent defined by

$$U_E^{\rm opt}(s)=-\left|U^{\rm opt}(s)\right|, \tag{A8}$$

with $\bar{\epsilon}$ in (A7) taken to be the average of the binding energies.

We now turn to the free binding limit, already described briefly in Sec. II. Here, the binding energy approaches zero and the ground state nucleon wave function becomes shallow, with an extended range, much larger than the range of the binding potential. Because binding is weak and the optical potential is shallow and smooth, the local momenta $k_\epsilon(s)$ and $k_\pi(s)$ are replaced by their asymptotic values and (45) is specialized to its single-nucleon form, $aL_0=1s=0$, $L_1=J$. Because the ground state nucleon wave function is smooth and the continuum nucleon wave function is nearly free, we take the Born limit for $F^J(R)$ in the nonlocal part of (45). Then the nonlocal integral

$$P^J_{0\epsilon}=\int dR\, R v_0(k_\pi(R))\psi_0(R)\bar{\psi}^*_{\epsilon J}(R)F^J(R)$$

becomes

$$P^J_{0\epsilon}\propto v_0(k_\pi)\psi_0(s)\delta(k_\pi-k_\epsilon), \tag{A9}$$

where the delta function is caused by momentum matching between F^J and $\bar{\psi}_{\epsilon J}$. The ϵ integral in (45) changes the $v_0(k_\epsilon)$ into a $v_0(k_\pi)$ and the $\bar{\psi}_{\epsilon J}(s)$ into a $F^J(s)$. This yields the free limit elastic Schrödinger equation

$$[T_\pi-t_J(s)]F^J(s)=2\pi^2 t_f(T_\pi^{\rm c.m.};k_\pi,k_\pi)\left|\psi_0(s)\right|^2F^J_f(s), \tag{A10}$$

where we have used (A3) and (A4). The energy argument of t_f, $T_\pi+\epsilon_0-\epsilon$, becomes $T_\pi^{\rm c.m.}=T_\pi-\epsilon_\pi$, the πN center-of-mass frame pion energy. Here ϵ_π is the nucleon energy at which the pion and nucleon momenta match. The $\bar{\nu}$ in (43b) implies that k_π in (A10) is also a center-of-mass frame quantity. We notice that Eq. (A10) for the free binding limit is immediately obtained from (A5) if ϵ_π is the closure energy.

[1]Some reviews are (a) M. M. Sternheim and R. R. Silbar, Annu. Rev. Nucl. Sci. 24, 249 (1974); (b) J. Hüfner, Phys. Rep. 21C, 1 (1975); (c) R. Barrett and D. Jackson *Nuclear Sizes and Structures* (Clarendon, Oxford, 1977), Sec. 10.4.1; (d) *Meson-Nuclear Physics-1976*, proceedings of the International Topical Conference on Meson-Nuclear Physics, Pittsburgh, edited by P. D. Barnes, R. A. Eisenstein, and L. S. Kisslinger (A. I. P., New York, 1976).

[2]E. H. Auerbach, D. M. Fleming, and M. M. Sternheim, Phys. Rev. 162, 1683 (1967); 171, 1781 (1968); M. M. Sternheim and E. H. Auerbach, Phys. Rev. Lett. 25, 1500 (1970).

[3]M. Krell and S. Barmo, Nucl. Phys. B20, 461 (1970).

[4]J. P. Dedonder, Nucl. Phys. A174, 251 (1971); A180, 472 (1972).

[5]R. H. Landau, S. C. Phatak, and F. Tabakin, Ann. Phys. (N.Y.) 78, 299 (1973); S. C. Phatak, F. Tabakin, and R. H. Landau, Phys. Rev. C 7, 1803 (1973); R. H. Landau, Phys. Lett. B57, 13 (1975); Ann. Phys. (N.Y.) 92, 205 (1975); Phys. Rev. C 15, 2127 (1977).

[6]L. A. Charlton and J. M. Eisenberg, Ann. Phys. (N.Y.) 63, 286 (1971).

[7]M. P. Locher, O. Steinmann, and N. Straumann, Nucl. Phys. B27, 598 (1971).

[8]L. S. Kisslinger, R. L. Burman, J. H. Koch, and M. M. Sternheim, Phys. Rev. C 6, 469 (1972).

[9]H. K. Lee and H. McManus, Nucl. Phys. A167, 257 (1971).

[10]E. A. Remler, Ann. Phys. (N.Y.) 67, 114 (1972).

[11]L. S. Kisslinger and F. Tabakin, Phys. Rev. C 9, 188 (1974).

[12]E. Kujawski, Nucl. Phys. A239, 467 (1975).

[13]D. I. Julius and C. Rodgers, Phys. Rev. C 12, 206 (1975).

[14]R. A. Friedenberg and D. L. Weiss, Phys. Rev. C 14, 204 (1976).

[15]M. Wakamatsu, Nucl. Phys. A312, 427 (1978).

[16]R. Mach, Nucl. Phys. A258, 513 (1976).
[17]D. J. Ernst, C. M. Shakin, and R. M. Thaler, Phys. Rev. C 9, 1374 (1974).
[18]L. C. Liu and C. M. Shakin, Phys. Rev. C 19, 129 (1979).
[19]W. R. Gibbs, A. T. Hess, and W. B. Kaufmann, Phys. Rev. C 13, 1982 (1976); W. R. Gibbs, B. F. Gibson, A. T. Hess, G. J. Stephenson, Jr., and W. B. Kaufmann, *ibid.* 13, 2433 (1976).
[20]D. Agassi and A. Gal, Ann. Phys. (N.Y.) 75, 56 (1973); 94, 184 (1975); D. Agassi, A. Gal, and V. Mandelzweig, *ibid.* 91, 194 (1975).
[21]L. S. Kisslinger and W. L. Wang, Phys. Rev. Lett. 30, 1071 (1973); Ann. Phys. (N.Y.) 99, 374 (1976).
[22]W. A. Friedman, Phys. Rev. C 12, 1294 (1975).
[23]G. E. Brown and W. Weise, Phys. Rep. 22C, 279 (1975); E. Oset and W. Weise, Phys. Lett. B77, 159 (1978).
[24]J. N. Ginocchio, Phys. Rev. C 17, 195 (1978).
[25]T. Kohmura, Nucl. Phys. B36, 228 (1972).
[26]J. Révai, Nucl. Phys. A205, 20 (1973).
[27]P. C. Tandy, E. F. Redish, and D. Bolle, Phys. Rev. C 16, 1924 (1977).
[28]C. Schmit, Nucl. Phys. A197, 449 (1972).
[29]M. G. Piepho and G. E. Walker, Phys. Rev. C 9, 1352 (1974).
[30]E. R. Siciliano and G. E. Walker, Phys. Rev. C 13, 257 (1976).
[31]J. P. Dedonder and C. Schmit, Phys. Lett. B65, 131 (1976).
[32]J. P. Maillet, J. P. Dedonder, and C. Schmit, Nucl. Phys. A271, 253 (1976).
[33]J. P. Maillet, J. P. Dedonder, and C. Schmit, Nucl. Phys. A316, 267 (1979).
[34]K. K. Bajaj and Y. Nogami, Phys. Rev. Lett. 34, 701 (1975); Ann. Phys. (N.Y.) 103, 141 (1977).
[35]R. H. Landau and A. W. Thomas, Phys. Lett. B61, 361 (1976); Nucl. Phys. A302, 461 (1978).
[36]R. D. Amado, F. Lenz, and K. Yazaki, Phys. Rev. C 18, 918 (1978).
[37]S. A. Gurvitz, J. P. Dedonder, and R. D. Amado, Phys. Rev. C 19, 142 (1979).
[38]M. Silver, Ph.D. thesis, University of Pittsburgh, 1979 (unpublished).
[39]N. Austern, J. P. Farrell, Jr., K. Kabir, and C. M. Vincent, Phys. Rev. C 18, 1577 (1978).
[40]F. Myhrer and D. S. Koltun, Phys. Lett. B46, 322 (1973).
[41]D. I. Julius, Ann. Phys. (N.Y.) 87, 17 (1974).
[42]E. Kujawski and M. Aitkin, Nucl. Phys. A221, 60 (1974).
[43]F. Myhrer, Nucl. Phys. A241, 524 (1975).
[44]I. R. Afnan and A. W. Thomas, Phys. Rev. C 10, 109 (1974).
[45]A. W. Thomas, Nucl. Phys. A258, 417 (1976).
[46]D. D. Brayshaw, Phys. Rev. C 11, 1196 (1975).
[47]R. M. Woloshyn, E. J. Moniz, and R. Aaron, Phys. Rev. C 13, 286 (1976).
[48]E. M. Ferreira, L. P. Rosa, and Z. D. Thome, Phys. Rev. C 16, 2353 (1977).
[49]N. Giraud, Y. Avishai, C. Fayard, and G. H. Lamot, Phys. Lett. B77, 141 (1978); Phys. Rev. C 19, 465 (1979).
[50]F. Lenz, Ann. Phys. (N.Y.) 95, 348 (1975).
[51]M. Hirata, F. Lenz, and K. Yazaki, Ann. Phys. (N.Y.) 108, 116 (1977).
[52]D. H. Herndon, A. Barbaro Galtieri, and A. H. Rosenfeld, LRL Report No. UCRL-20030, πN, 1970 (unpublished), CERN Experimental Solution.
[53]F. Tabakin, private communication.
[54]M. A. Nagarajan, Nucl. Phys. A196, 34 (1972); N. K. Glendenning, and M. A. Nagarajan, *ibid.* A236, 13 (1974).
[55]M. L. Goldberger and K. M. Watson, *Collision Theory* (Wiley, New York, 1964), Sec. 6.8.
[56]John M. Blatt and Victor F. Weisskopf, *Theoretical Nuclear Physics* (Wiley, New York, 1952), Sec. VIII. 2.a.
[57]M. Thies, Phys. Lett. B63, 39 (1976).
[58]Mikkel B. Johnson, private communication.
[59]F. G. Perey and B. Buck, Nucl. Phys., 32, 353 (1962).
[60]T. E. O. Ericson and J. Hüfner, Phys. Lett. B33, 601 (1970).
[61]J. E. Sedlak and W. A. Friedman, Phys. Rev. C 16, 2306 (1977).
[62]A. S. Clough, G. K. Turner, B. W. Allardyce, C. J. Batty, D. J. Baugh, W. J. McDonald, R. A. J. Riddle, L. H. Watson, M. E. Cage, G. J. Pyle, and G. T. A. Squier, Nucl. Phys. B76, 15 (1974).
[63]J. P. Albanèse, J. Arvieux, E. Boschitz, C. H. Q. Ingram, L. Pflug, C. Wiedner, and J. Zichy, Phys. Lett. B73, 119 (1978); Q. Ingram, E. Boschitz, L. Pflug, J. Zichy, J. P. Albanese, and J. Arvieux, *ibid.* B76, 173 (1978).